Scientific Research Publishing

Computational Molecular Bioscience, 2024, 14, 59-123
https://www.scirp.org/journal/cmb
ISSN Online: 2165-3453
ISSN Print: 2165-3445

Molecular Docking Studies of Botanical Beverage Mix Berries (LIFEGREEN™) against Breast Cancer Cells from Targeted Protein 1QQG, 7B5Q & 7B5O & Uterine Fibroid from Targeted Protein 2AYR, 6T41 & 3GRF

Ummi Shahieda Lazaroo Bt Zurrein Shah Lazaroo[1,2,3,4], Navanithan Sivanananthan[4], Chua Kia How[5,6,7]

[1]Department of Scientific Research of Lifetree Asia Sdn Bhd, Selangor, Malaysia
[2]Department of Scientific Research of Lifetree Biotech Sdn Bhd, Selangor, Malaysia
[3]Department of Research and Development of Nutrimedt Sdn Bhd, Selangor, Malaysia
[4]Faculty of Health & Life Sciences, Management & Science University, Selangor, Malaysia
[5]Lifetree Asia Sdn Bhd, Selangor, Malaysia
[6]Lifetree Biotech Sdn Bhd, Selangor, Malaysia
[7]Nutrimedt Sdn Bhd, Selangor, Malaysia
Email: mishalazaroo@gmail.com, 2209nava@gmail.com, kia2200@gmail.com

How to cite this paper: Shahieda Lazaroo Bt Zurrein Shah Lazaroo, U., Sivanananthan, N. and How, C.K. (2024) Molecular Docking Studies of Botanical Beverage Mix Berries (LIFEGREEN™) against Breast Cancer Cells from Targeted Protein 1QQG, 7B5Q & 7B5O & Uterine Fibroid from Targeted Protein 2AYR, 6T41 & 3GRF. *Computational Molecular Bioscience*, **14**, 59-123.
https://doi.org/10.4236/cmb.2024.142004

Received: April 24, 2024
Accepted: June 10, 2024
Published: June 13, 2024

Abstract

Fibroids, also called leiomyomas or myomas, are communal tumors of the muscle or uterine wall that affect about 20% of females who are of reproductive age. They can look as if singly or in clusters, and they often cease to grow after menopause. Fibroids can be classified as intramural, sub serosal, pedunculated, or submucosal based on where they are positioned in the uterus. Although fibroids are benign, they can grow quickly and cause a range of symptoms, such as pelvic pressure, heavy menstrual flow, and infertility. As a result, fibroids are a main reason behind hysterectomy surgeries. The majority of cases of breast cancer are ductal and lobular cancers, making it the second utmost common cancer in women international. Gene mutations like those in BRCA1 or BRCA2 knowingly raise the risk of breast and other cancers, typically with an earlier cancer onset. Cancer risk is influenced by a complex interplay of genetic abnormalities, environmental factors, and lifestyle selections. Further research into these relations is domineering. Although they are common in uterine leiomyomas, especially multiple leiomyomas, MED12 mutations do not significantly correlate with tumor size. These mutations have also been noticed in smooth muscle tumors and leiomyosarcomas, two

other types of uterine cancer. The identification of MED12 mutations as the sole genetic abnormality originates in leiomyomas raises the opportunity of a role in the genesis of cancer. 10% - 15% of women who are of reproductive age have endometriosis, which grants serious difficulties because of its chronic nature and range of clinical symptoms. Even after effective surgeries, issues reoccur often, adding to the enormous financial burden. The effects of MED12 mutations have been experiential in recent studies examining the molecular causes of endometriosis-associated infertility, which have shown anomalies in cellular connections and signaling cascades. Computational techniques were used in this study to investigate LifeGreen™'s potential to prevent uterine fibroids and breast cancer. The efficacy of LifeGreen™ as a preventive measure or a treatment for common gynecological matters was examined and modeled. We investigated the mechanisms underlying LifeGreen™'s benefits in the treatment of uterine fibroids and breast cancer using computational techniques. Our research contributes to our understanding of its potential therapeutic benefits for women's health.

Keywords

Uterine Fibroid, Breast Cancer, Molecular Docking, IRS Protein, BRCA1, BRCA2, MED12-a, Endometriosis

1. Introduction

1.1. LifeGreen™

LifeGreen™ Cactus Powder is known as a highly concentrated cactus extract which made using 22 different types of fruit and vegetable extracts, Italian mixed berries, and TRUEBROC® broccoli seed extract, a US-patented ingredient, Oxxynea® is a popular French health drink. According to studies, cactus polysaccharides having the ability to boost immunity and inhibit abnormal cell developments when consumed over time. In addition, Truebroc® broccoli seed extract promotes aberrant cell death, reduces abnormal cell blood supply, and prevents abnormal cell reproduction and spread. **Figure 1** shows the packaging of the LifeGreen™ Beverage [1].

1.2. Ingredients and Benefits

LifeGreen™ contains Italian Premium Mixed Berries (Blueberry, Blackcurrant, Raspberry, Elderberry, Red Grape, Strawberry, Cranberry), Cactus Powder, Oxxynea® (Green Tea Extract, Red Grape Extract, White Grape Extract, Bilberry, Carrot, Grapefruit, Papaya, Pineapple, Strawberry, Apple, Apricot, Cherry, Orange, Broccoli, Green Cabbage, Onion, Garlic, Olive, Cucumber, Blackcurrant, Tomato, Asparagus), TRUEBROC® broccoli seed extract, and immune deficiencies include fatigue and weakness, allergies, and the need to restore immunity. Moreover, LifeGreen™'s ingredients, particularly Cactus Powder, have been extensively researched and studied for their anticancer effects. **Figure 2** shows the picture of LifeGreen™ Beverage drink [1].

Figure 1. Lifegreen™ Beverage sachet and packaging [1].

Figure 2. Lifegreen™ Beverage drink [1].

1.3. Cancer Cell Growth

The body creates molecules are known as growth factors, which govern cell division. Growth factors occur in a number of types and each operates differently. Some growth factors advise cells on how to specialize and what type of cell they should become. Some cause cell division and proliferation to generate new cells. Cells can be told to cease growing or die. Growth factors operate by binding to cell surface receptors. This sends a signal to the cell's inside, initiating a sequence of complex chemical reactions. There are multiple different growth factors [2]. These include epidermal growth factor (EGF), vascular endothelial growth factor

(VEGF), platelet-derived endothelial growth factor (PDGF), and fibroblast growth factor (FGF), which all regulate cell growth. Each growth factor works by attaching to its corresponding cell surface receptor. For example, epidermal growth factor (EGF) interacts with the EGFR. Tyrosine Kinases are chemical messengers (enzymes) that control cells' capacity to divide and grow. Similar to an "on-off" switch feature, Tyrosine kinase is activated when a growth factor attaches to a cell's surface. This will prompt cell division as shown in **Figure 3** [2].

1.4. Uterine Fibroids

Fibroids, also known as leiomyoma or myoma, are frequent tumors that develop in the uterine wall or muscle. Fibroids in women of their reproductive years can present as single or multiple growths. Fibroids are uncommon in women who have not yet started menstruation, although they afflict around 20% of women of reproductive age. Usually, growth slows after menopause [3]. Fibroids can be classified into various types based on where they exist. The submucosal fibroid is a fibroid that usually develops inside the uterus while intramural fibroid is a fibroid that develops within the musculature of the uterine wall. Moreover, subserosa fibroid is known as a uterine fibroid that protrudes from the body. Lastly, a fibroid with a stalk that extent from the uterus into the pelvis or else discovered inside the inner uterine cavity and extends through cervix is known as pedunculated fibroid. **Figure 4** shows the locations of the various types of fibroids [4].

Despite their benign nature, they can grow rapidly and dramatically [5]. They produce heavy and irregular menstrual bleeding (HMB), which leads to severe anemia, dysmenorrhea, pelvic pressure and discomfort, urinary incontinence, dyspareunia, infertility, premature labor, and recurrent early and late pregnancy losses [6]. More than 70% of women have UFs, with only around 30% experiencing

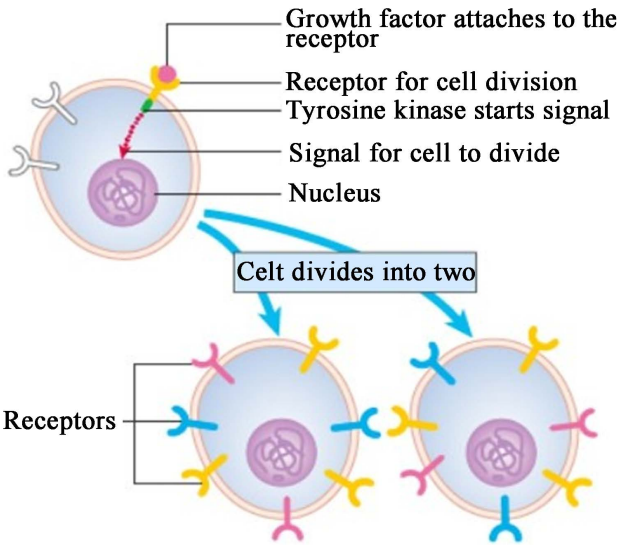

Figure 3. The cancer cells growth factor that affects the body [2].

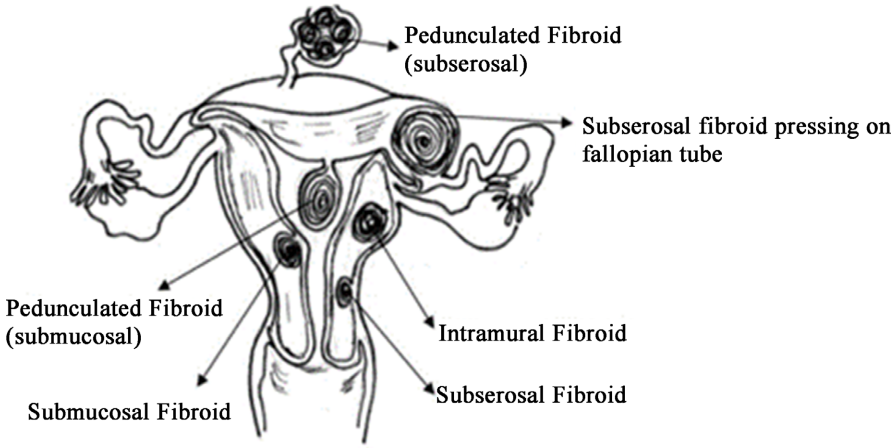

Figure 4. The common locations for uterine fibroid to occur [4].

symptoms, making UFs the most common clinical cause for hysterectomy, which removes a woman's capacity to produce early [7].

1.5. Breast Cancer Cells (IRS-1)

Breast cancer is the world's second most frequent illness, affecting more women than any other malignancy. The two most common types of breast cancer are ductal and lobular. In situ (localized to a single location), ductal and lobular cancers account for 85% - 90% and 8% of all breast cancers, respectively. In addition, aggressive inflammatory breast cancers exist, as do invasive ductal and lobular tumors. Although chemotherapy has been demonstrated to improve breast cancer patients' survival rates, a significant minority of individuals only have a brief response to the treatment before succumbing to metastatic disease. IRS1 has been shown to enhance breast cancer cell growth rather than preventing metastasis [8]. **Figure 5** shows the process of IRS-1 occurring before metastasis happen in which responsible for the growth of breast cancer cell [9].

1.6. BRCA 1 & BRCA 2

People protecting injurious variants in BRCA1 or BRCA2 genes aspect significantly higher risks of emerging various cancers, together with breast, ovarian, fallopian tube, and primary peritoneal cancers [10]. The incidence of these mutations significantly rises the lifetime risk of cancer onset, with pretentious people often facing earlier age of cancer diagnosis equated to the general population. While BRCA mutations are sturdily associated with increased cancer risk, the extent of risk variability amongst carriers is inclined by various factors [10]. These issues include environmental contacts, lifestyle choices, hormonal effects, and genetic modifiers that may interrelate with BRCA mutations to modulate cancer susceptibility. In spite of extensive research, some of these factors remain somewhat characterized, highlighting the need for further investigation into the complex interplay between genetic and environmental determinants of cancer risk [11].

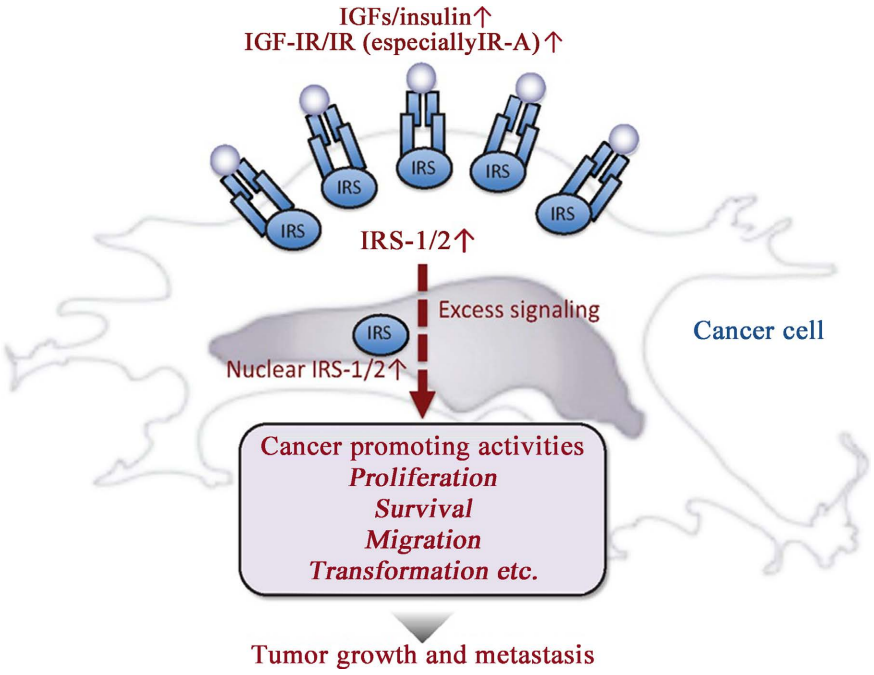

Figure 5. The process of IRS-1 occurring before metastasis happens causes breast cancer cell growth.

1.7. MED12-a

Tumors did not exhibit more than one mutation, and previous research did not address the MED12 mutation status of multiple leiomyomas in one patient. Multiple uterine leiomyomas appeared to have a higher incidence of MED12 mutations compared to single uterine leiomyomas (72.73% versus 59.26%), although this difference was not statistically significant [12]. Moreover, patients with multiple leiomyomas exhibited smaller mean sizes of leiomyomas significantly, consistent with previous research. Nearly twofold difference in MED12 mutation frequency between multiple and single uterine leiomyomas from a cohort of 122 patients. However, they could not establish a significant association between MED12 mutation and tumor size [12]. Therefore, larger sample sizes are required to evaluate the relationship between MED12 mutation frequency and the number or size of uterine leiomyomas. MED12 mutation has also been detected in other uterine tumors such as leiomyosarcomas and smooth muscle tumors of uncertain malignant potential, but not in tumors of other organs. Interestingly, breast fibroadenoma also harbored highly frequent MED12 mutations. Whole exome sequencing revealed no genes other than MED12 mutation in MED12 mutation-positive and -negative leiomyomas, suggesting that MED12 mutation alone may be sufficient for leiomyoma tumorigenesis [12].

1.8. Endometriosis

Endometriosis is a multifaceted gynecological state affecting 10% - 15% of reproductive-age females and around 70% of women facing persistent pelvic pain. While the ovaries and pelvic peritoneum are the primary sites of endometriotic

lesions, they can also patent in various other locations inside the body [13]. The etiologic of endometriosis-associated pain remains poorly unspoken, with inflammation broadly believed to play a significant role. Despite fruitful surgical interventions, recurrence of symptoms is communal, underscoring the chronic nature of the condition. Endometriosis poses a substantial economic burden, particularly in countries like India, with costs estimated at approximately 1 to 2 lakhs per affected woman. The participation of structures such as the uterosacral ligaments, posterior vaginal wall, rectovaginal space, intestines, and urinary system is frequently experiential in endometriosis cases. Various studies have explored the molecular mechanisms underlying endometriosis-associated infertility, highlighting factors such as apoptosis, cell cycle alterations, and oxidative stress in granulosa cells. Moreover, recent research endeavors have sought to elucidate the role of MED12 mutations in endometriosis pathogenesis, revealing disruptions in cellular interactions and signaling pathways [13].

2. Methodology

LifeGreen™ uses proteomic computing to identify compounds that can interact with IRS-1 (breast cancer cells) as well as BRCA 1 and 2 - 1QQG, 7B5Q & 7B5O and endometriosis and mutated Med-a (uterine fibroid)-2AYR, 3GRF & 6T41 proteins [14]. Furthermore, additional research and investigations on each effective molecule with the highest binding energy and its advantages to human health. **Figure 6** shows the general methodology of this research while **Figure 7**

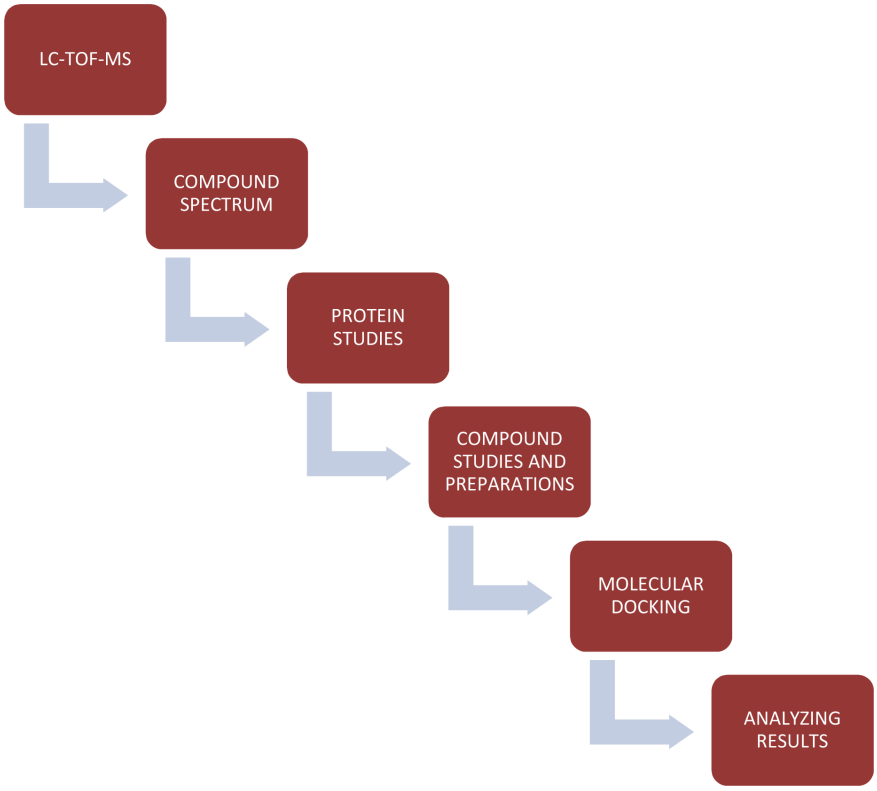

Figure 6. Overview of the whole methodology

until Figure 10 shows the in-depth methodology.

2.1. Phase 1: Metabolomics Analysis

In Figure 7, in chromatography process, separation was performed using Thermo Scientific C18 column (Acclaim™ Polar Advantage II, 3 × 150 mm, 3 um particle size) on an UltiMate 3000 UHPLC system (Dionex) [15]. Gradient elution was performed at flow rate of 0.4 ml/min and 40˚C column temperature using H_2O + 0.1% Formic Acid (A) and 100% ACN (B) with 22 minutes total run time. The injection volume of sample was 5 ul. The gradient started at 5% B (0 - 3 min); 80% B (3 - 10 min); 80% B (10 - 15 min) and 5% B (15 - 22 min). For mass-spectrophotometry, sample is analyzed with positive ionization parameter [15], Table 1.

In data processing steps, the accurate mass data of the molecular ions, provided by the TOF analyzer, were processed by Compass Data Analysis software

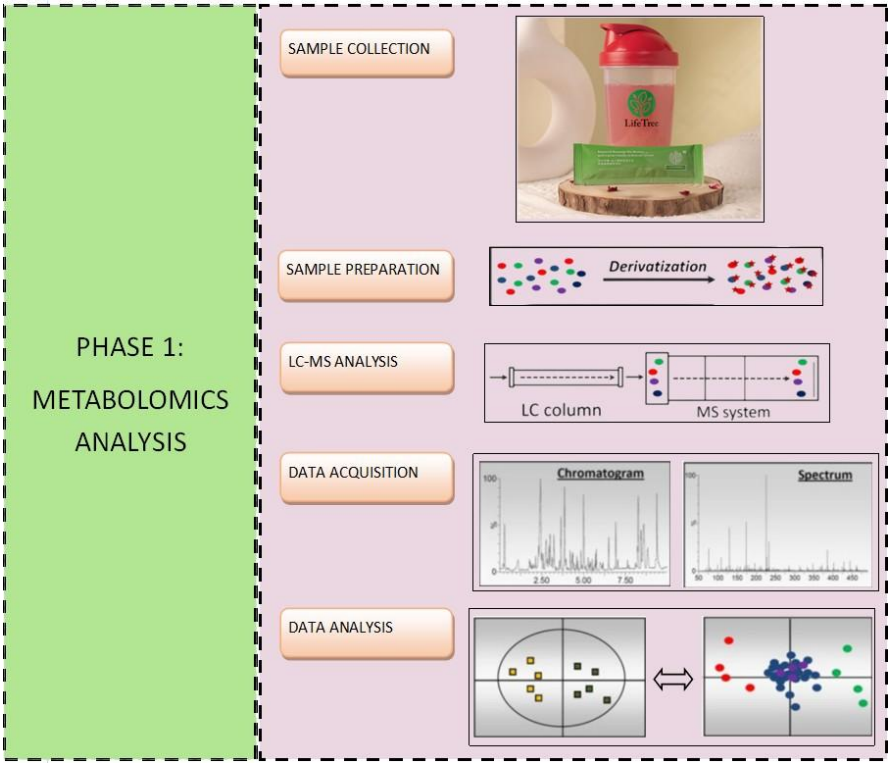

Figure 7. Phase 1: Metabolomics Analysis.

Table 1. Positive mode ionization.

Acquisition Parameter					
Source Type	***ESI***	**Ion Polarity**	***Positive***	**Set Nebulizer**	**2.0**
Focus	Active	Set Capillary	4500 V	Set Dry Heater	300˚C
Scan Begin	50 m/z	Set End Place Offset	−500 V	Set Dry Gas	8.0 l/min
Scan End	1500 m/z	Set Collision Cell RF	200.0 Vpp	Set Divert Valve	Waste

(Bruker Daltonik GmbH). Further process by using metfrag (In silico fragmentation for computer assisted identification of metabolite mass spectra) in order to pull out the list of compound present in each peak presented by LC-MS/TOF [16] *gi-bin/portal.py#welcome*.

2.2. Phase 2: Compound Analysis

Before proceeding with the analysis, each compound underwent meticulous quality control procedures employing ZoBio by NMR, ensuring the integrity and reliability of subsequent results. Following this initial step, the compounds were subjected to an array of sophisticated analyses aimed at elucidating their properties and functions. Significance testing was employed to discern meaningful patterns and deviations within the dataset, shedding light on potential biological implications. Quantitation-pattern recognition techniques were applied to discern quantitative relationships and trends within the data, facilitating a deeper understanding of compound behavior. Compound assignment methodologies were utilized to accurately identify and classify each compound, ensuring precise cataloguing and characterization. Finally, functional assessment protocols were implemented to assess the biological activities and potential applications of the compounds, providing valuable insights for further research, **Figure 8**.

2.3. Phase 3: Protein Analysis

During this third phase of the study **Figure 9**, an extensive protein analysis was undertaken utilizing resources available on the Protein Data Bank (PDB) https://www.rcsb.org/ website [17]. This involved a meticulous examination of protein structures and relevant data to glean insights into the molecular

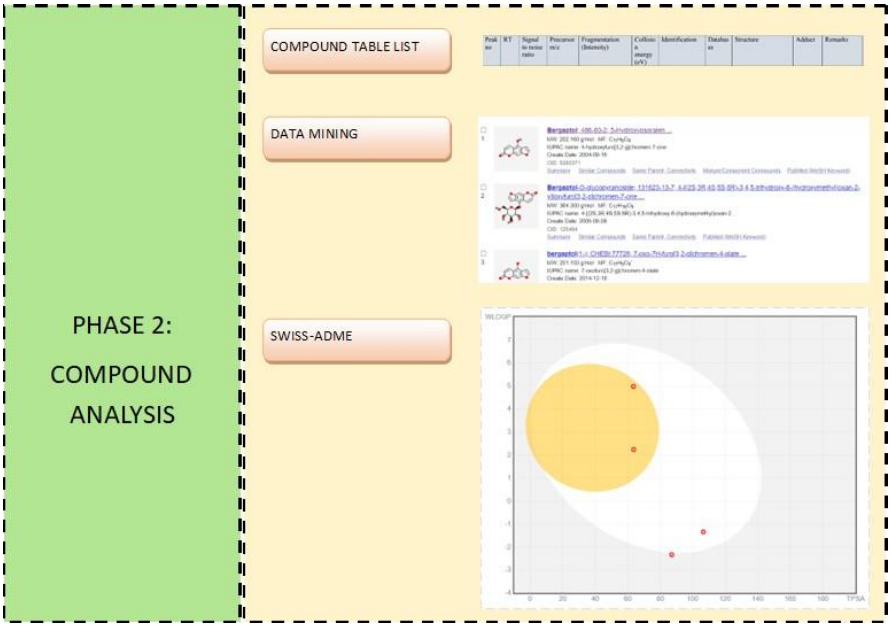

Figure 8. Phase 2: Compound analysis.

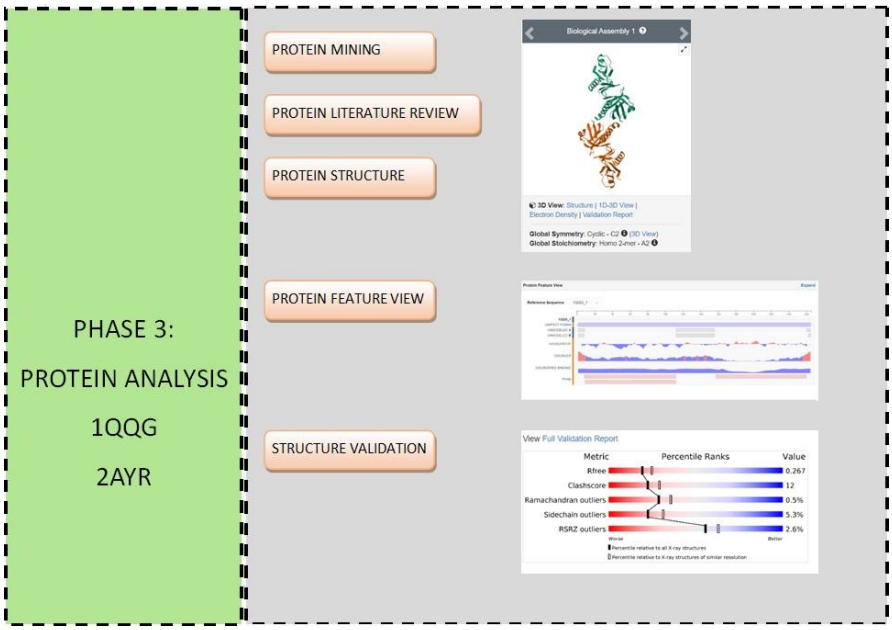

Figure 9. Phase 3: Protein analysis of 1QQG, 2AYR, 3GRF, 6T41, 7B5Q and 7B5O.

Table 2. Breast cancer and uterine fibroid flow.

Breast Cancer		Uterine Fibroid	
IRS-1	BRCA1 & BRCA 2	Endometriosis	MED a (mutated)
IRS1 was found to promote breast cancer cell proliferation	XPB & XPD TFIIH	Tissue lining grows outside the uterus	CDK 8/Cyclin C.
1QQG	7B5Q & 7B5O	2AYR	3RGF & 6T41

underpinnings of the investigated conditions. To augment our understanding, a thorough literature review was conducted. This involved delving into published studies and scientific literature to identify and elucidate the roles of specific proteins implicated in breast cancer and uterine fibroids. By synthesizing information from various sources, we aimed to pinpoint key proteins associated with these diseases, providing a comprehensive foundation for our research. **Table 2** serves as a comprehensive repository of the gathered results pertaining to both breast cancer and uterine fibroids. This tabulated data offers a detailed overview of the proteins identified and their respective implications in the pathogenesis of these conditions. Through meticulous documentation and analysis, we aim to uncover potential biomarkers and therapeutic targets, contributing to the advancement of diagnostics and treatment strategies for breast cancer and uterine fibroids.

2.4. Phase 4 and Phase 5: Protein-Ligand Interactions and Molecular Docking

In **Figure 10**, proteomic molecular docking represents a sophisticated computational approach used in the field of proteomics to predict and analyses the

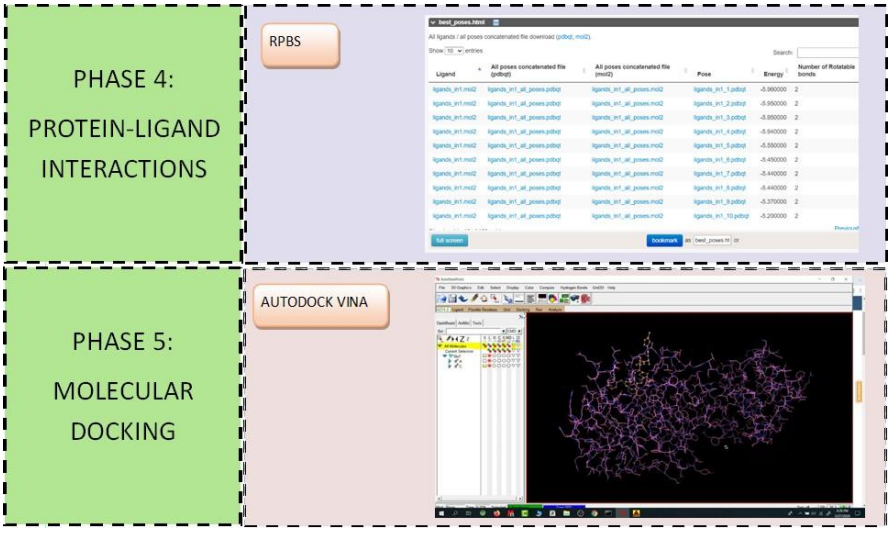

Figure 10. Phase 4: Protein-Ligand Interaction (RPBS) and Phase 5: Molecular Docking.

interactions between proteins and other molecules, Achilles Blind Docking Server, https://bio-hpc.ucam.edu/achilles/. This method integrates principles from both proteomics and molecular docking, leveraging computational algorithms to simulate and predict the binding affinity and spatial orientation of proteins with various ligands, substrates, or inhibitors. The process typically begins with the identification of target proteins of interest through proteomic techniques such as mass spectrometry or protein microarrays. Once the target proteins are identified, molecular docking algorithms are employed to simulate the binding interactions between these proteins and small molecules, peptides, or other proteins. These docking algorithms use complex scoring functions and search algorithms to explore the conformational space and predict the most energetically favorable binding poses between the proteins and their ligands. By analyzing these predicted binding conformations, researchers can gain valuable insights into the molecular mechanisms underlying protein-ligand interactions, including the identification of key binding residues and structural determinants. Proteomic molecular docking holds significant promise for various applications in drug discovery, structural biology, and systems pharmacology. It enables the screening of large compound libraries to identify potential drug candidates or lead compounds that modulate the activity of target proteins implicated in diseases. Additionally, it facilitates the elucidation of protein-protein interaction networks and signaling pathways, providing valuable insights into complex biological processes and disease mechanisms.

3. Results

3.1. LC-TOF-MS

In Figure 11, the chemical composition of LifeGreen™ samples, LC-TOF MS analysis emerged as a pivotal investigative tool, yielding a comprehensive compound spectrum graph delineating the peaks indicative of molecular entities

Acquisition Parameter

Source Type	ESI	Ion Polarity	Positive	Set Nebulizer	2.0 Bar
Focus	Not active	Set Capillary	4500 V	Set Dry Heater	300 °C
Scan Begin	50 m/z	Set End Plate Offset	-500 V	Set Dry Gas	8.0 l/min
Scan End	1500 m/z	Set Collision Cell RF	200.0 Vpp	Set Divert Valve	Waste

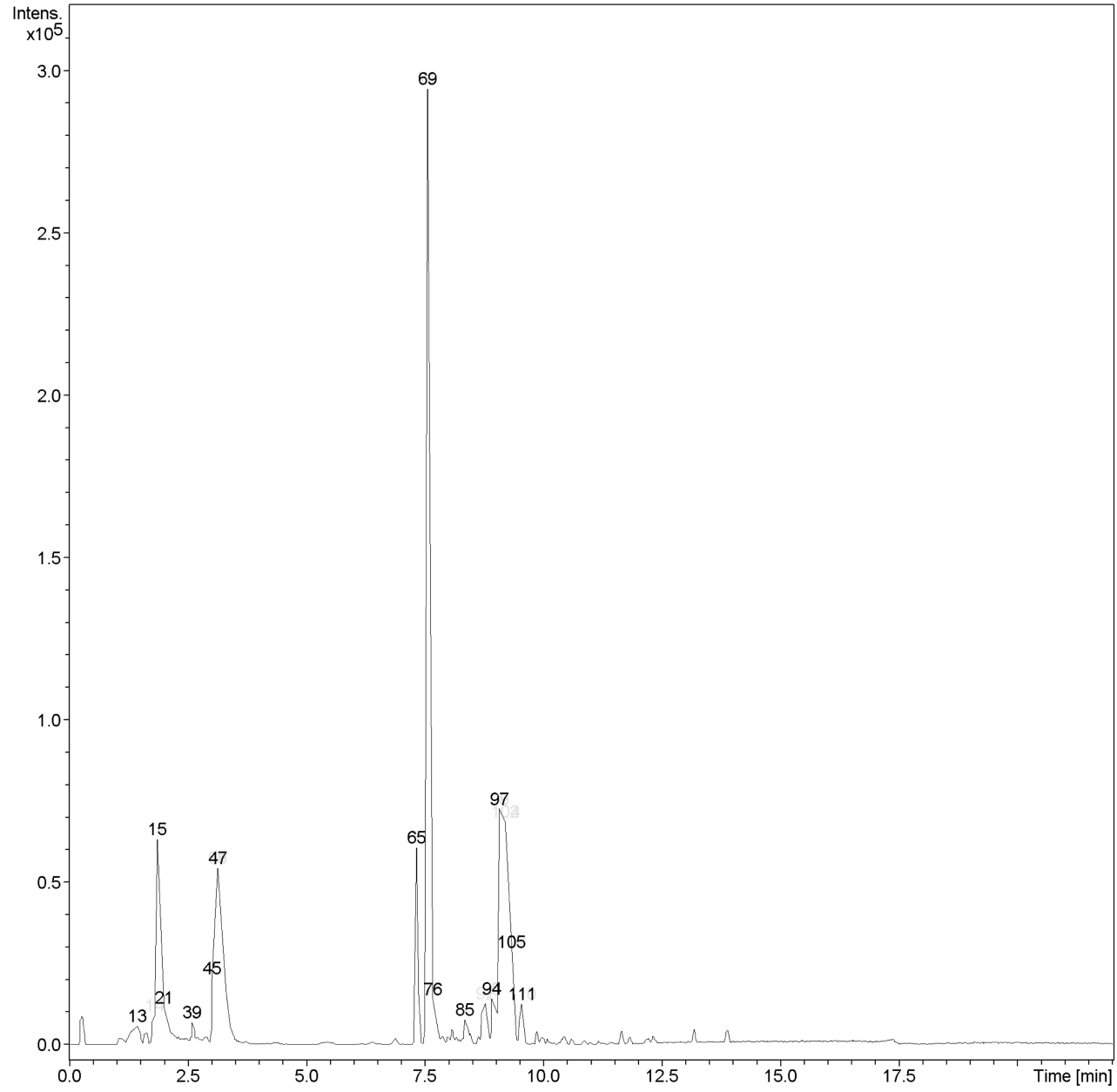

Figure 11. Shows the compound spectrum graph and its peaks.

present within the samples. Notably, the analysis revealed approximately 140 distinct compounds, with varying degrees of detectability attributable to the inherent limitations posed by sample composition and instrumental sensitivity. Within this array, certain compounds were readily discernible, while others remained undetected, a phenomenon attributed to the relatively sparse population of compounds within the samples.

In our examination of the compound spectrum graph, each peak was charac-

terized by its corresponding retention time (RT) in minutes, intensity, signal-to-noise ratio, maximum mass-to-charge ratio (m/z), and area under the peak. These parameters collectively provided insights into the abundance, purity, and spectral characteristics of the identified compounds. Furthermore, to augment our understanding of the molecular identities associated with the observed peaks, collision energy (eV) values were assigned to selected peaks, facilitating subsequent tandem mass spectrometry (MS/MS) analyses.

To unveil the chemical identities corresponding to the observed peaks, we employed the computational tools afforded by MetFrag. Leveraging the spectral information encapsulated within the LC-TOF MS data, MetFrag facilitated the deconvolution of complex spectra, enabling the retrieval and annotation of putative compounds associated with each peak, Table 3.

Table 3. Shows the compound spectrum list of LifeGreen™.

#	RT [min]	Area	Int. Type	I	S/N	Chromatogram	Max. m/z
1	0.3	14319	MolFeatur	2290	25.4		158.9642
2	1.1	7552	MolFeatur	364	8.1		892.302
3	1.1	24660	MolFeatur	858	4.9		1297.4271
4	1.1	16541	MolFeatur	814	3.9		1135.3787
5	1.1	25047	MolFeatur	2021	7.7		325.1159
6	1.1	13410	MolFeatur	364	3.9		1378.9585
7	1.1	21376	MolFeatur	1240	5.8		973.3256
8	1.1	11438	MolFeatur	889	9.9		487.165
9	1.1	17711	MolFeatur	1216	13.5		649.221
10	1.3	46188	MolFeatur	2300	3.2		125.9873
11	1.3	11554	MolFeatur	595	3.3		153.0319
12	1.4	41690	MolFeatur	2138	7.8		143.998
13	1.4	78569	AutoMS(n)	5811	66.7	AutoMSn (242.0010)	218.9853
14	1.8	50134	AutoMS(n)	9113	116	AutoMSn (147.0776)	147.0777
15	1.9	49668	AutoMS(n)	5860	73	AutoMSn (309.1324)	325.1181
16	1.9	222361	AutoMS(n)	14,913	72.4	AutoMSn (163.0613)	325.118
17	1.9	462886	AutoMS(n)	63,448	664.5	AutoMSn (325.1166)	325.1181
18	1.9	59405	AutoMS(n)	5810	63	AutoMSn (203.0533)	325.118
19	1.9	3860	MolFeatur	2800	49.8		265.0968
20	1.9	781734	MolFeatur	41,601	425.2		325.118
21	2	79661	AutoMS(n)	8555	88.6	AutoMSn (365.1092)	163.0609
22	2	11871	MolFeatur	8484	96.9		365.1103
23	2.1	66073	MolFeatur	1004	10.8		145.0516

Continued

24	2.1	170832	MolFeatur	1939	21.2		163.0615
25	2.2	188364	MolFeatur	1939	21.2		163.0614
26	2.2	35326	MolFeatur	459	3.7		973.3298
27	2.2	41514	MolFeatur	489	4.5		1054.3589
28	2.2	50877	MolFeatur	684	7.6		1135.3881
29	2.3	14168	MolFeatur	283	3.1		1236.9162
30	2.3	46769	MolFeatur	563	6.3		1216.9174
31	2.4	7917	MolFeatur	984	9.3		497.1519
32	2.4	6183	MolFeatur	612	6.6		198.0778
33	2.4	49982	MolFeatur	534	3		1297.4404
34	2.5	23467	MolFeatur	383	3.3		1378.9711
35	2.5	18898	MolFeatur	345	3.8		1387.9728
36	2.5	11851	MolFeatur	318	3.5		1460
37	2.5	8619	MolFeatur	319	3.8		1469.0016
38	2.6	12885	MolFeatur	1764	13.7		307.0905
39	2.6	29720	AutoMS(n)	7065	70.1	AutoMSn (268.1092)	136.064
40	2.6	4844	MolFeatur	356	4		117.0568
41	2.6	17930	MolFeatur	954	10.4		163.062
42	2.7	24200	MolFeatur	1679	8.2		294.1604
43	2.8	24504	MolFeatur	749	3.3		261.0418
44	2.8	7757	MolFeatur	343	3.9		1423.7855
45	3	44717	AutoMS(n)	6350	70.9	AutoMSn (130.0523)	215.0195
46	3.1	19762	MolFeatur	8840	62.6		230.994
47	3.1	131922	AutoMS(n)	8910	93	AutoMSn (230.9921)	215.0192
48	3.1	316934	AutoMS(n)	24,784	315.4	AutoMSn (407.0478)	215.0193
49	3.1	749494	AutoMS(n)	54,493	349.9	AutoMSn (215.0178)	215.0192
50	3.1	102957	AutoMS(n)	7504	67.5	AutoMSn (193.0361)	215.0192
51	3.1	103373	AutoMS(n)	6945	60.7	AutoMSn (308.0244)	215.0191
52	3.1	95222	MolFeatur	4404	48.9		193.0371
53	3.2	301781	MolFeatur	12,438	138.2		215.0194
54	3.3	697424	MolFeatur	20,160	149.4		215.0191
55	3.7	10392	MolFeatur	1057	8.2		302.0911
56	3.7	8383	MolFeatur	909	7.5		166.0876
57	4.1	8535	MolFeatur	321	3.6		328.1426
58	4.4	11022	MolFeatur	710	4.9		277.1583

Continued

59	5.4	12378	MolFeatur	548	4.7		460.0383
60	5.4	20326	MolFeatur	925	10.3		358.1004
61	5.4	14422	MolFeatur	737	8.2		196.0475
62	6.4	11266	MolFeatur	873	9.5		311.1273
63	6.5	6705	MolFeatur	361	4		361.1123
64	7	3669	MolFeatur	315	3.5		389.1815
65	7.3	247093	AutoMS(n)	60,926	887.7	AutoMSn (310.1649)	251.0943
66	7.4	3888	MolFeatur	306	3.4		896.4008
67	7.5	5669	MolFeatur	416	4.6		476.2284
68	7.6	1454	MolFeatur	396	6.8		703.351
69	7.6	297019	AutoMS(n)	60,619	549	AutoMSn (589.2497)	295.1332
70	7.6	1613847	AutoMS(n)	294,260	3251.2	AutoMSn (295.1298)	295.1332
71	7.6	27313	AutoMS(n)	5368	44.5	AutoMSn (611.2289)	295.1332
72	7.6	36156	MolFeatur	17,093	379.8		590.255
73	7.6	1860691	MolFeatur	99,937	41.2		295.1331
74	7.7	8045	MolFeatur	5178	44.1		287.0581
75	7.7	94945	AutoMS(n)	9837	82.1	AutoMSn (279.0470)	295.1315
76	7.7	39453	AutoMS(n)	5249	51.3	AutoMSn (449.1033)	295.1315
77	7.7	143129	MolFeatur	6626	22.2		279.0498
78	7.8	39909	MolFeatur	1495	7.3		211.06
79	7.9	5869	MolFeatur	451	10		1156.4916
80	8	6146	MolFeatur	844	6.9		453.2078
81	8	8300	MolFeatur	459	5.1		247.0831
82	8	7534	MolFeatur	1513	16.8		195.0889
83	8.2	11008	MolFeatur	1359	30.2		765.2588
84	8.2	4727	MolFeatur	631	6.7		635.2532
85	8.3	49149	AutoMS(n)	7874	68.1	AutoMSn (362.2406)	362.2436
86	8.3	28410	AutoMS(n)	6319	66.5	AutoMSn (340.2600)	322.2509
87	8.4	16121	MolFeatur	1257	12		481.1332
88	8.6	2674	MolFeatur	317	3.5		787.2362
89	8.7	16551	MolFeatur	846	9.4		141.0545
90	8.8	3726	MolFeatur	1266	4.9		429.1734
91	8.8	103448	AutoMS(n)	12,920	116.5	AutoMSn (475.3227)	475.3273
92	8.8	52265	AutoMS(n)	6608	60.4	AutoMSn (453.3422)	453.3441
93	8.9	11754	MolFeatur	723	8		625.1779

Continued

94	8.9	76886	AutoMS(n)	11,827	104.2	AutoMSn (566.4229)	566.4304
95	8.9	115283	AutoMS(n)	14,400	107.5	AutoMSn (588.4059)	588.4125
96	8.9	57648	AutoMS(n)	9152	93.9	AutoMSn (283.7180)	588.4104
97	9.1	410677	AutoMS(n)	72,826	766.7	AutoMSn (340.2600)	114.0925
98	9.1	212347	AutoMS(n)	39,912	260.3	AutoMSn (679.5096)	679.5153
99	9.1	175923	AutoMS(n)	28,600	176.1	AutoMSn (701.4907)	701.4972
100	9.1	855268	MolFeatur	32,414	37.6		114.0925
101	9.2	257033	MolFeatur	9413	209.2		701.4972
102	9.2	549469	AutoMS(n)	69,035	633.7	AutoMSn (396.8013)	396.8049
103	9.2	137634	AutoMS(n)	17,220	114.8	AutoMSn (814.5751)	814.5812
104	9.2	122930	AutoMS(n)	15,509	123.3	AutoMSn (792.5921)	396.8049
105	9.3		AutoMS(n)	5379		AutoMS (n): TIC + MS2 (340.2587)	
106	9.3	207392	AutoMS(n)	28,786	404.8	AutoMSn (274.2738)	274.2773
107	9.3	50477	AutoMS(n)	6733	71.2	AutoMSn (318.2989)	274.277
108	9.5	7283	MolFeatur	638	6.2		155.047
109	9.5	26104	MolFeatur	12,699	61.1		183.0786
110	9.5	75436	AutoMS(n)	12,781	152.9	AutoMSn (183.0768)	183.0786
111	9.5	34410	AutoMS(n)	7875	97.2	AutoMSn (290.2694)	183.0787
112	9.5	13638	MolFeatur	7844	151.7		290.2727
113	10	18573	MolFeatur	2371	3.6		389.2515
114	10.1	8421	MolFeatur	1406	15.6		304.3024
115	10.1	3945	MolFeatur	618	4.9		318.3028
116	10.4	8374	MolFeatur	998	7.1		188.0479
117	10.4	21705	MolFeatur	2542	3.8		447.2916
118	10.9	12476	MolFeatur	1335	5.2		505.3321
119	11.3	2349	MolFeatur	273	3		235.1688
120	11.5	8109	MolFeatur	621	6		343.2974
121	11.6	25151	MolFeatur	3668	40.8		288.2552
122	11.8	12750	MolFeatur	2517	36.2		225.1943
123	12.3	37695	MolFeatur	1329	14.8		239.1618
124	12.3	15554	MolFeatur	2306	25.6		199.1688
125	12.3	12451	MolFeatur	1074	8.8		209.1528
126	13	4050	MolFeatur	693	3.8		421.2309
127	13.2	25382	MolFeatur	3875	43.1		383.2033
128	13.2	115665	MolFeatur	544	6		506.3295

Continued

129	13.9	31914	MolFeatur	4401	48.9	425.2118
130	13.9	6244	MolFeatur	835	9.3	441.1855
131	14.2	5321	MolFeatur	726	8.1	370.2006
132	15	277893	MolFeatur	832	6.1	907.7663
133	15	138295	MolFeatur	484	3.9	404.3161
134	15.4	9501	MolFeatur	870	8	398.2321
135	16.2	324760	MolFeatur	933	5.5	758.5641
136	16.3	398562	MolFeatur	1304	6.2	603.5311
137	16.6	54641	MolFeatur	379	3.8	782.5625
138	16.7	257755	MolFeatur	1157	9	756.5476
139	17.3	43661	MolFeatur	317	3.4	897.7209
140	17.3	432817	MolFeatur	1504	10.7	923.74

3.2. MetFrag

In **Table A1**, through the utilization of MetFrag, a comprehensive compilation of compounds was extracted from each designated peak within the compound spectrum graph generated via LC-TOF MS analysis of the LifeGreen™ samples. These compounds were meticulously identified, characterized, and annotated, facilitating the elucidation of their chemical nature and potential functional attributes [18].

Each identified compound was assigned a canonical SMILES (Simplified Molecular Input Line Entry System) representation, serving as a concise yet comprehensive descriptor of its molecular structure. Additionally, molecular formulas were determined, encapsulating the precise arrangement of atoms constituting each compound, thus providing crucial insights into their elemental composition and stoichiometry [18]. The benefits and potential applications associated with each identified compound were elucidated, leveraging existing knowledge and literature resources. These benefits encompassed a diverse array of domains, including pharmaceuticals, agriculture, food science, cosmetics, and environmental remediation, among others [18].

By integrating the structural information derived from canonical SMILES notation and molecular formulas with the contextual understanding of their functional properties, a holistic perspective on the chemical constituents present within the LifeGreen™ samples was attained, **Table 4**.

3.3. LifeGreen™ Compounds

3.3.1. Swiss-ADME

The compiled list of 117 compounds extracted from the LC-TOF MS analysis of LifeGreen™ samples underwent comprehensive evaluation via SwissADME, a robust computational platform designed to assess various pharmacokinetic and pharmacodynamic parameters crucial for drug discovery and development [19].

Table 4. Shows list of compounds in LifeGreen™.

COMPOUND NAME	*FORMULA*	*SMILES*
Phenethyl anthranilate	C15H15NO2	C1=CC=C(C=C1)CCOC(=O)C2=CC=CC=C2N
D-glutamine	C5H10N2O3	C(CC(=O)N)C(C(=O)O)N
Citrus red 2	C18H16N2O3	COC1=CC(=C(C=C1)OC)N=NC2=C(C=CC3=CC=CC=C32)O
1,5-Anhydro-D-fructose	C6H10O5	C1C(=O)C(C(C(O1)CO)O)O
Bis-D-fructose 2',1:2,1'-dianhydride	C12H20O10	C1C2(C(C(C(O2)CO)O)O)OCC3(O1)C(C(C(O3)CO)O)O
Bergaptol	C11H6O4	C1=CC(=O)OC2=CC3=C(C=CO3)C(=C21)O
Bergapten	C12H8O4	COC1=C2C=CC(=O)OC2=CC3=C1C=CO3
Isobergaptol	C11H6O4	C1=CC(=O)OC2=C1C(=CC3=C2C=CO3)O
Abscisic acid	C15H20O4	CC1=CC(=O)CC(C1(C=CC(=CC(=O)O)C)O)(C)C
(-)-Abscisic acid		CC1=CC(=O)CC(C1(C=CC(=CC(=O)O)C)O)(C)C
(+)-8'-Hydroxyabscisic acid	C15H20O5	CC1=CC(=O)CC(C1(C=CC(=CC(=O)O)C)O)(C)CO
(+)-abscisic acid beta-D-glucopyranosyl ester	C21H30O9	CC1=CC(=O)CC(C1(C=CC(=CC(=O)OC2C(C(C(C(O2)CO)O)O)O)C)O)(C)C
D-Fructofuranose 1,2":2,3"-dianhydride	C12H20O10	C1C2(C(C(C(O2)CO)O)O)OC3C(C(OC3(O1)CO)CO)O
10-Hydroxycamptothecin	C20H16N2O5	CCC1(C2=C(COC1=O)C(=O)N3CC4=C(C3=C2)N=C5C=CC(=CC5=C4)O)O
2-(Hydroxymethyl)pentanedioic acid	C6H10O5	C(CC(=O)O)C(CO)C(=O)O
Adenosin		C1=NC(=C2C(=N1)N(C=N2)C3C(C(C(O3)CO)O)O)N
4-hydroxycoumarin		C1=CC=C2C(=C1)C(=CC(=O)O2)O
Alpha-beta-Dihydroresveratrol	C14H14O3	C1=CC(=CC=C1CCC2=CC(=CC(=C2)O)O)O
Casticin	C19H18O8	COC1=C(C=C(C=C1)C2=C(C(=O)C3=C(C(=C(C=C3O2)OC)OC)O)OC)O
4-nitrophenylalanine	C9H10N2O4	C1=CC(=CC=C1CC(C(=O)O)N)[N+](=O)[O-]
citrate	C6H8O7	C(C(=O)O)C(CC(=O)O)(C(=O)O)O
3-Hydroxy-3-Carboxy-Adipic Acid	C7H10O7	C(CC(CC(=O)O)(C(=O)O)O)C(=O)O
(1R,2S)-1-hydroxybutane-1,2,4-tricarboxylic acid	C7H10O7	C(CC(=O)O)C(C(C(=O)O)O)C(=O)O
(2R)-dihomocitric acid	C8H12O7	C(CC(=O)O)CC(CC(=O)O)(C(=O)O)O
(-)-Threo-isodihomocitric acid	C8H12O7	C(CC(C(C(=O)O)O)C(=O)O)CC(=O)O
(2R)-trihomocitric acid	C9H14O7	C(CCC(CC(=O)O)(C(=O)O)O)CC(=O)O
1-Hydroxyhexane-1,2,6-tricarboxylate	C9H14O7	C(CCC(=O)O)CC(C(C(=O)O)O)C(=O)O
Riccionidin A	C15H9O6+	C1=C2C=C3C(=C4C(=CC(=CC4=[OH+])O)O3)OC2=CC(=C1O)O
Scopoletin	C10H8O4	COC1=C(C=C2C(=C1)C=CC(=O)O2)O
2-Deoxy-D-ribose 5-phosphate	C5H11O7P	C1C(C(OC1O)COP(=O)(O)O)O

Continued

cyanidin	C15H11O6+	C1=CC(=C(C=C1C2=[O+]C3=CC(=CC(=C3C=C2O)O)O)O)O
Dinoflagellate luciferin	C33H40N4O6	CCC1=C(NC(=C1C)CC2C(=C(C(=O)N2)C)C=C)CC3=C(C4=C(N3)C(=C5C(C(C(N5)C(=O)O)C)CCC(=O)O)CC4=O)C
(3S,4S,5E)-4-(2-carboxyethyl)-5-[2-({5-[(3-ethenyl-4-methyl-5-oxo-2,5-dihydro-1H-pyrrol-2-yl)methyl]-3-ethyl-4-methyl-1H-pyrrol-2-yl}methyl)-3-methyl-4,5-dioxo-4,5-dihydrocyclopenta[b]pyrrol-6(1H)-ylidene]-3-methyl-L-proline	C33H38N4O7	CCC1=C(NC(=C1C)CC2C(=C(C(=O)N2)C)C=C)CC3=C(C4=C(N3)C(=C5C(C(C(N5)C(=O)O)C)CCC(=O)O)C(=O)C4=O)C
N-Glycosyl-L-asparagine	C10H18N2O8	C(C1C(C(C(C(O1)NC(=O)CC(C(=O)O)N)O)O)O)O
Hesperidin	C28H34O15	CC1C(C(C(C(O1)OCC2C(C(C(C(O2)OC3=CC(=C4C(=O)CC(OC4=C3)C5=CC(=C(C=C5)OC)O)O)O)O)O)O)O)O
Methyl hesperidin	C29H36O15	CC1C(C(C(C(O1)OCC2C(C(C(C(O2)OC3=CC(=C4C(=O)CC(OC4=C3)C5=CC(=C(C=C5)OC)OC)O)O)O)O)O)O)O
Arbutin	C12H16O7	C1=CC(=CC=C1O)OC2C(C(C(C(O2)CO)O)O)O
alpha-Arbutin	C12H16O7	C1=CC(=CC=C1O)OC2C(C(C(C(O2)CO)O)O)O
Methylarbutin	C13H18O7	COC1=CC=C(C=C1)OC2C(C(C(C(O2)CO)O)O)O
Quercitrin	C21H20O11	CC1C(C(C(C(O1)OC2=C(OC3=CC(=CC(=C3C2=O)O)O)O)C4=CC(=C(C=C4)O)O)O)O)O
3'',5''-Dihydroxyflavanone	C15H12O4	C1C(OC2=CC=CC=C2C1=O)C3=CC(=CC(=C3)O)O
(2S)-2',7-Dimethoxy-3',5-dihydroxyflavanone	C17H16O6	COC1=CC(=C2C(=O)CC(OC2=C1)C3=C(C(=CC=C3)O)OC)O
Orientin	C21H20O11	C1=CC(=C(C=C1C2=CC(=O)C3=C(O2)C(=C(C=C3O)O)C4C(C(C(C(O4)CO)O)O)O)O)O
Evocarpine	C23H33NO	CCCCC=CCCCCCCCC1=CC(=O)C2=CC=CC=C2N1C
(Z)-1-Methyl-2-(tridec-8-en-1-yl)quinolin-4(1H)-one	C23H33NO	CCCCC=CCCCCCCCC1=CC(=O)C2=CC=CC=C2N1C
Aspalathin	C21H24O11	C1=CC(=C(C=C1CCC(=O)C2=C(C=C(C(=C2O)C3C(C(C(C(O3)CO)O)O)O)O)O)O)O
1-Stearoylglycerophosphocholine	C26H55NO7P+	CCCCCCCCCCCCCCCCCC(=O)OCC(COP(=O)(O)OCC[N+](C)(C)C)O
1-Octadecanoyl-sn-glycero-3-phosphocholine	C26H54NO7P	CCCCCCCCCCCCCCCCCC(=O)OCC(COP(=O)([O-])OCC[N+](C)(C)C)O
Sinigrin	C10H17NO9S2	C=CCC(=NOS(=O)(=O)O)SC1C(C(C(C(O1)CO)O)O)O
Spirilloxanthin	C42H60O2	CC(=CC=CC(=CC=CC(=CC=CC=C(C)C=CC=C(C)C=CC=C(C)C=CCC(C)(C)OC)C)C)C=CCC(C)(C)OC
Aridanin	C38H61NO8	CC(=O)NC1C(C(C(OC1OC2CCC3(C(C2(C)C)CCC4(C3CC=C5C4(CCC6(C5CC(CC6)(C)C)C(=O)O)C)C)C)CO)O)O
1-Hexadecanoyl-2-(9Z-octadecenoyl)-sn-glycero-3-phosphoethanolamine	C39H76NO8P	CCCCCCCCCCCCCCCC(=O)OCC(COP(=O)(O)OCCN)OC(=O)CCCCCCCC=CCCCCCCCC

Continued

Hexadecasphinganine	C16H35NO2	CCCCCCCCCCCCCCC(C(CO)N)O
Phytosphingosine	C18H39NO3	CCCCCCCCCCCCCCCC(C(C(CO)N)O)O
Piperonal	C8H6O3	C1OC2=C(O1)C=C(C=C2)C=O
Lupanine	C15H24N2O	C1CCN2CC3CC(C2C1)CN4C3CCCC4=O
Flavanone	C15H12O2	C1C(OC2=CC=CC=C2C1=O)C3=CC=CC=C3
2-hydroxy flavone	C22H26ClNO4	CC1=CC=C(C=C1)C2=CC(=O)C3=C(O2)C=C(C=C3)OCC(CNC(C)C)O.Cl
Dihydrostillbene base	C14H12O2	C1=CC(=CC=C1C=CC2=CC=C(C=C2)O)O
5-Sulfosalicylate	C7H6O6S	C1=CC(=C(C=C1S(=O)(=O)O)C(=O)O)O
Glabranin	C20H20O4	CC(=CCC1=C(C=C(C2=C1OC(CC2=O)C3=CC=CC=C3)O)O)C
2-Deoxy-scyllo-inososе	C6H10O5	C1C(C(C(C(C1=O)O)O)O)O
Acetanilide	C8H9NO	CC(=O)NC1=CC=CC=C1
Niridazole	C6H6N4O3S	C1CN(C(=O)N1)C2=NC=C(S2)[N+](=O)[O-]
Citrinin	C13H14O5	[H][C@]1(C)OC=C2C(O)=C(C(O)=O)C(=O)C(C)=C2[C@]1([H])C
Aspartame	C14H18N2O5	COC(=O)C(CC1=CC=CC=C1)NC(=O)C(CC(=O)O)N
epsilon-Caprolactam	C6H11NO	C1CCC(=O)NCC1
cis-3-(3-Carboxyethenyl)-3,5-cyclohexadiene-1,2-diol	C9H10O4	C1=CC(C(C(=C1)C=CC(=O)O)O)O
Isobavachalcone	C20H20O4	CC(=CCC1=C(C=CC(=C1O)C(=O)C=CC2=CC=C(C=C2)O)O)C
Glabridin	C20H20O4	CC1(C=CC2=C(O1)C=CC3=C2OCC(C3)C4=C(C=C(C=C4)O)O)C
Mycocyclosin	C18H16N2O4	C1C2C(=O)NC(CC3=CC(=C(C=C3)O)C4=C(C=CC1=C4)O)C(=O)N2
2,3-Dehydro-UWM6	C19H16O5	CC1=CC(=O)C2C3=C(C(=O)CC2(C1)O)C(=C4C(=C3)C=CC=C4O)O
Prazepam	C19H17ClN2O	C1CC1CN2C(=O)CN=C(C3=C2C=CC(=C3)Cl)C4=CC=CC=C4
(-)-Phaseollinisoflavan	C20H20O4	CC1(C=CC2=C(O1)C=CC(=C2O)C3CC4=C(C=C(C=C4)O)OC3)C
Phaseollidin	C20H20O4	CC(=CCC1=C(C=CC2=C1OC3C2COC4=C3C=CC(=C4)O)O)C
Bis-D-fructose 2”,1:2,1”-dianhydride	C12H20O10	C1C2(C(C(C(O2)CO)O)O)OCC3(O1)C(C(C(O3)CO)O)O
2-Dehydro-3-deoxy-D-fuconate	C6H10O5	CC(C(CC(=O)C(=O)O)O)O
2-Dehydro-3-deoxy-L-rhamnonate	C6H10O5	CC(C(CC(=O)C(=O)O)O)O
2-Dehydro-3-deoxy-L-fuconate	C6H10O5	CC(C(CC(=O)C(=O)O)O)O
Diethyl pyrocarbonate	C6H10O5	CCOC(=O)OC(=O)OCC

Continued

3,6-Anhydro-alpha-L-galactopyranose	C6H10O5	C1C2C(C(O1)C(C(O2)O)O)O
Eugenol quinone methide	C10H10O2	COC1=CC(=CC=C)C=CC1=O
Methyl cinnamate	C10H10O2	COC(=O)C=CC1=CC=CC=C1
p-Methoxycinnamaldehyde	C10H10O2	COC1=CC=C(C=C1)C=CC=O
2-Hydroxymethylserine	C4H9NO4	C(C(CO)(C(=O)O)N)O
2-Phenylacetamide	C8H9NO	C1=CC=C(C=C1)CC(=O)N
4-Hydroxy-L-threonine	C4H9NO4	C(C(C(C(=O)O)N)O)O
N-Benzylformamide	C8H9NO	C1=CC=C(C=C1)CNC=O
Adenine	C5H5N5	C1=NC2=C(N1)C(=NC=N2)N
(E)-Phenylacetaldoxime	C8H9NO	C1=CC=C(C=C1)CC=NO
(Z)-Phenylacetaldehyde oxime	C8H9NO	C1=CC=C(C=C1)CC=NO
Dibenzo[1,4]dioxin-2,3-dione	C12H6O4	C1=CC=C2C(=C1)OC3=CC(=O)C(=O)C=C3O2
5-Deoxyribose-1-phosphate	C5H11O7P	CC1C(C(C(O1)OP(=O)(O)O)O)O
2-Deoxy-D-ribose 1-phosphate	C5H11O7P	C1C(C(OC1OP(=O)(O)O)CO)O
1-Deoxy-D-xylulose 5-phosphate	C5H11O7P	CC(=O)C(C(COP(=O)(O)O)O)O
3,5-Dinitroguaiacol	C7H6N2O6	COC1=C(C=C(C=C1O)[N+](=O)[O-])[N+](=O)[O-]
2-(5”-Methylthio)pentylmalic acid	C10H18O5S	CSCCCCCC(CC(=O)O)(C(=O)O)O
3-(5”-Methylthio)pentylmalic acid	C10H18O5S	CSCCCCCC(C(C(=O)O)O)C(=O)O
3-(m-Aminophenyl)-2-(p-methoxyphenyl)acrylonitrile	C16H14N2O	COC1=CC=C(C=C1)C(=CC2=CC(=CC=C2)N)C#N
Glycophymoline	C16H14N2O	COC1=NC(=NC2=CC=CC=C21)CC3=CC=CC=C3
Flindersiachromone	C17H14O2	C1=CC=C(C=C1)CCC2=CC(=O)C3=CC=CC=C3O2
Arborine	C16H14N2O	CN1C2=CC=CC=C2C(=O)N=C1CC3=CC=CC=C3
4,4”-Methylenediphenyl diisocyanate	C15H10N2O2	C1=CC(=CC=C1CC2=CC=C(C=C2)N=C=O)N=C=O
Methaqualone	C16H14N2O	CC1=CC=CC=C1N2C(=NC3=CC=CC=C3C2=O)C
Triamiphos	C12H19N6OP	CN(C)P(=O)(N1C(=NC(=N1)C2=CC=CC=C2)N)N(C)C
2-[3-Ethyl-5-(4-methoxyphenyl)-1H-pyrazol-4-yl]phenol	C18H18N2O2	CCC1=C(C(=NN1)C2=CC=C(C=C2)OC)C3=CC=CC=C3O
(2-Butylbenzofuran-3-yl)(4-hydroxyphenyl)ketone	C19H18O3	CCCCC1=C(C2=CC=CC=C2O1)C(=O)C3=CC=C(C=C3)O
Tutin	C15H18O6	CC(=C)C1C2C(C3(C4(CO4)C5C(C3(C1C(=O)O2)O)O5)C)O
3-Methoxy-4-hydroxyphenylglycolaldehyde	C9H10O4	COC1=C(C=CC(=C1)C(C=O)O)O
(R)-3-(4-Hydroxyphenyl)lactate	C9H10O4	C1=CC(=CC=C1CC(C(=O)O)O)O
3,4-Dihydroxyphenylpropanoate	C9H10O4	C1=CC(=C(C=C1CCC(=O)O)O)O
2”,6”-Dihydroxy-4”-methoxyacetophenone	C9H10O4	CC(=O)C1=C(C=C(C=C1O)OC)O

Continued

3-(4-Hydroxyphenyl)lactate	C9H10O4	C1=CC(=CC=C1CC(C(=O)O)O)O
Homovanillate	C9H10O4	COC1=C(C=CC(=C1)CC(=O)O)O
3-(2,3-Dihydroxyphenyl)propanoate	C9H10O4	C1=CC(=C(C(=C1)O)O)CCC(=O)O
Mannitol	C6H14O6	C(C(C(C(C(CO)O)O)O)O)O
D-Sorbitol	C6H14O6	C(C(C(C(C(CO)O)O)O)O)O

This systematic scrutiny aimed to discern the compounds exhibiting favorable pharmacological properties conducive to combatting breast cancer and uterine fibroids, thus offering promising avenues for therapeutic intervention. Within this rigorous evaluation framework, several key metrics were scrutinized, including compliance with Lipinski's Rule of Five, a pivotal criterion for predicting oral bioavailability and permeability of potential drug candidates. Additionally, lead-likeness, hydrogen bond donor and acceptor counts, and bioavailability scores were meticulously examined, offering valuable insights into the compounds' drug-like properties and therapeutic potential [19]. By leveraging the insights gleaned from SwissADME analysis, compounds exhibiting optimal pharmacokinetic profiles and bioavailability were identified as prime candidates for further investigation and therapeutic development. These compounds, characterized by their propensity to permeate biological barriers, maintain favorable drug-like properties, and exhibit high bioavailability, hold promise in the targeted management and mitigation of breast cancer and uterine fibroids [19]. The systematic integration of LC-TOF MS analysis, compound identification, and SwissADME evaluation represents a pivotal step towards the rational design and discovery of novel therapeutics aimed at addressing the unmet clinical needs associated with breast cancer and uterine fibroids. Through this concerted effort, the identification of lead compounds with enhanced efficacy and safety profiles heralds a significant stride towards personalized and precision medicine approaches tailored to combat these debilitating diseases [19].

3.3.2. RPBS

Following the initial filtration process employing SwissADME, which identified 51 compounds with potential efficacy against breast cancer and uterine fibroids, a subsequent analysis utilizing RPBS was conducted to evaluate rotatable bonds and energy profiles. This additional scrutiny yielded a refined subset of 34 compounds, each characterized by optimal structural flexibility and energetics conducive to molecular docking studies [20]. The RPBS assessment provided crucial insights into the molecular dynamics of the selected compounds, elucidating their ability to adopt diverse conformations and facilitating efficient interactions with target biomolecules implicated in disease pathogenesis [20]. By prioritizing compounds with favorable rotatable bond counts and energy profiles, this iterative screening process enhances the rational selection of lead candidates poised for further preclinical evaluation, **Table 5** [20].

Table 5. Shows down streaming results from RPBS tools.

COMPOUND NAME	RB	E (1QQG)	E (2AYR)	E(7B	E (6T41)	E (3GRF)	E (7B5O)
	<5	<−5					
Bergaptol	0	−7.9	−8.4	−8.7	−8.9	−8.8	−8.6
Bergapten	1	−7.6	−8	−8.9	−9.1	−8.9	−8.1
Isobergaptol	0	−8.2	−8.6	−8.7	−8.6	−8.6	−8.6
Abscisic acid	3	−7.9	−7.7	−8.9	−8.6	−7.9	−7.9
(-)-Abscisic acid	3	−8	−7.5	−8.9	−8.6	−8.5	−7.9
(+)-8'-Hydroxyabscisic acid	4	−7.4	−7.3	−8.5	−8	−8.1	−8
(+)-abscisic acid beta-D-glucopyranosyl ester	6	−9.6	−9.2	−9.7	−9.4	−8.9	−9.5
10-Hydroxycamptothecin	1	−11.1	−11.4	−12.4	−12.9	−10.4	−11.4
4-hydroxycoumarin	0	−7.5	−7.4	−8.1	−7.5	−7.9	−7.4
Alpha-beta-Dihydroresveratrol	3	−8.2	−7.8	−9.4	−9.2	−8.4	−9
Casticin	5	−9	−8.4	−8.8	−8.7	−8	−9.1
Scopoletin	1	−7	−7.3	−8.2	−7.9	−7.8	−7.5
Methylarbutin	4	−7.8	−8	−8.4	−8.2	−7.7	−8.5
3",5"-Dihydroxyflavanone	1	−9.5	−9.3	−10.3	−10.4	−9.4	−9.9
(2S)-2',7-Dimethoxy-3',5-dihydroxyflavanone	3	−8.9	−8.9	−9.8	−9.9	−8.9	−9.3
Lupanine	0	−8.8	−9	−10.1	−10.1	−8.4	−9.8
Flavanone	1	−9.4	−9.3	−10.4	−10.3	−10	−10.2
5-Sulfosalicylate	2	−7.2	−7.5	−7.4	−7.3	−6.7	−7.3
Glabranin	3	−9.1	−9.6	−10.8	−10.6	−9.6	−10.5
Niridazole	2	−6.6	−7	−6.7	−6.9	−6.8	−6.5
Citrinin	1	−8.3	−8.9	−9.1	−9.4	−9.8	−8.9
Aspartame	9	−7.5	−7.1	−7.8	−8.1	−7.6	−7.5
cis-3-(3-Carboxyethenyl)-3,5-cyclohexadiene-1,2-diol	2	−5.3	−5.3	−6.3	−5.8	−5.5	−5.6
Glabridin	1	−10.2	−11.1	−10.8	−12.3	−11	−10.7
Mycocyclosin	0	−11.1	−11.8	−12.7	−12.8	−12.3	−12.1
2,3-Dehydro-UWM6	0	−10.3	−10.5	−11.6	−11.9	−10.7	−11.6
Prazepam	3	−9.4	−9.9	−10.5	−10.5	−9.3	−10.3
(-)-Phaseollinisoflavan	1	−10.1	−11	−10.3	−12.4	−12.1	−10.6
Phaseollidin	2	−9.6	−10.1	−10.8	−10.8	−10	−10.4
Diethyl pyrocarbonate	6	−4.9	−5	−4.6	−5	−5.1	−5.1
Eugenol quinone methide	2	−6.2	−6.6	−7.3	−6.9	−7.1	−6.7
Methyl cinnamate	3	−6.6	−6.4	−7	−6.9	−7	−6.8

Continued

p-Methoxycinnamaldehyde	3	−6.4	−6.1	−6.9	−6.7	−6.8	−6.7
Dibenzo[1,4]dioxin-2,3-dione	0	−9.4	−9.2	−10.6	−9.7	−10.7	−9.4
3,5-Dinitroguaiacol	3	−6.2	−7	−7.1	−6.7	−6.8	−6.9
2-(5”-Methylthio)pentylmalic acid	9	−5.7	−5.7	−6	−5.9	−6	−5.4
3-(5”-Methylthio)pentylmalic acid	9	−4.9	−5.4	−6.6	−5.9	−6.3	−6.3
3-(m-Aminophenyl)-2-(p-methoxyphenyl)acrylonitrile	3	−8.2	−8.2	−7.6	−7.6	−8.2	−7.7
Glycophymoline	3	−8.8	−9.5	−10.5	−10.5	−10.1	−10.4
Flindersiachromone	3	−9.2	−9.4	−11	−10.5	−10.1	−10.5
Arborine	2	−9.2	−9.3	−10.8	−10	−9.7	−10.2
Methaqualone	1	−8.8	−9.6	−10.5	−10.3	−10.2	−9.9
Triamiphos	4	−7.5	−7.9	−8.1	−7.8	−7.6	−7.8
2-[3-Ethyl-5-(4-methoxyphenyl)-1H-pyrazol-4-yl]phenol	4	−8.4	−9	−8.5	−9.1	−9	−8.5
(2-Butylbenzofuran-3-yl)(4-hydroxyphenyl)ketone	5	−8	−7.1	−8.1	−8	−8.3	−8.3
Tutin	1	−8.6	−8.9	−9.1	−9.5	−8.6	−9
3-Methoxy-4-hydroxyphenylglycolaldehyde	3	−6.1	−6.7	−6.7	−6.5	−6.7	−6.5
(R)-3-(4-Hydroxyphenyl)lactate	3	−6.8	−6.9	−7.3	−7.4	−6.9	−7
2”,6”-Dihydroxy-4”-methoxyacetophenone	2	−6.3	−6.5	−6.3	−6.8	−6.9	−6.8
3-(4-Hydroxyphenyl)lactate	3	−6.6	−7	−7.3	−7.4	−7.2	−7
Homovanillate	3	−6.2	−7.1	−7.1	−6.9	−7.1	−6.8

Out of the initial pool of 34 compounds, only 22 demonstrated the remarkable capability to bind with all six protein diseases associated with both breast cancer and uterine fibroid. This subset of compounds exhibits broad-spectrum activity, indicating their potential to target multiple pathological pathways implicated in the progression of these diseases. Their ability to interact with diverse protein targets underscores their versatility and promise as candidate therapeutics [20]. In contrast, the remaining 12 compounds displayed a more selective binding profile, interacting with a subset of two to four protein diseases. While these compounds may exhibit efficacy against specific disease subtypes or pathways, their narrower spectrum of activity suggests a more targeted mode of action. Despite this selectivity, these compounds still hold considerable therapeutic potential and merit further investigation for their specific applications in breast cancer and uterine fibroid management [20].

3.3.3. Dogsitescorer

Dogsitescorer, a specialized computational tool, is employed to discern the

highest binding energy exhibited by potential compounds against protein targets implicated in breast cancer and uterine fibroid pathogenesis. Subsequently, coordinates corresponding to the identified binding sites are extracted from the output generated by Dogsitescorer [21]. These coordinates play a pivotal role in elucidating the precise molecular interactions between the candidate compounds and their respective protein targets. By pinpointing the specific binding sites on the protein surfaces, these coordinates provide valuable insights into the molecular mechanisms underpinning the observed binding affinities [21].

Furthermore, the coordinates obtained from Dogsitescorer serve as crucial input parameters for subsequent molecular docking simulations [21]. Leveraging advanced computational algorithms, molecular docking studies enable the prediction of the binding modes and affinities of the candidate compounds within the protein binding sites, offering valuable predictive insights into their therapeutic potential. Through the iterative integration of computational tools such as Dogsitescorer and molecular docking simulations, the identification of lead compounds with optimal binding energies and favorable interaction profiles against protein targets associated with breast cancer and uterine fibroids is facilitated. This systematic approach enhances the rational design and optimization of novel therapeutics aimed at mitigating the progression of these debilitating diseases [21].

3.3.4. Molecular Docking - Achilles Blind Docking Server

The 34 identified compounds, targeting breast cancer and uterine fibroid-associated protein diseases, underwent comprehensive molecular docking simulations using the ACHILLES BLIND DOCKING SERVER [22]. This state-of-the-art computational tool facilitated the exploration of compound-protein interactions across multiple protein targets, providing valuable insights into their binding affinities and binding site preferences. Through the blind docking approach employed by ACHILLES, the compatibility between each compound and the diverse array of protein targets associated with breast cancer and uterine fibroids was systematically evaluated. By considering multiple protein structures representative of different disease states, this approach enabled a comprehensive assessment of compound efficacy across various pathological contexts [22].

Furthermore, the molecular docking simulations facilitated the identification of potential binding sites within the protein coordinates for each compound. The number and distribution of these binding sites served as critical indicators of compound versatility and potential therapeutic efficacy. Compounds exhibiting a higher propensity to bind at multiple locations within the protein coordinates were deemed particularly promising, as they may exert broader therapeutic effects and target diverse disease mechanisms [22]. By integrating the insights gleaned from molecular docking simulations across multiple protein targets, a comprehensive understanding of compound-protein interactions and their potential implications for breast cancer and uterine fibroid management was attained, **Table 6**.

Table 6. Shows the number of locations within protein coordinate set by dogsitescorer's energy binding with a total residue > −6.

COMPOUND NAME	ID	NUMBER OF LOCATION WITHIN COORDINATE TOTAL RESIDUE (>−6)					
		1QQG	2AYR	3GRF	6T41	7B5Q	7B5O
Isobergaptol	10198122	1	1	1	6	6	6
10-Hydroxycamptothecin	97226	3	2	2	4	3	6
Casticin	5315263	1	2	1	4	5	6
3",5"-Dihydroxyflavanone	11954216	3	1	1	9	3	6
(2S)-2',7-Dimethoxy-3',5-dihydroxyflavanone	102066377	2	2	2	6	4	7
Lupanine	91471	1	2	1	4	3	3
Flavanone	10251	2	2	1	4	4	6
Glabranin	124049	2	2	2	5	2	6
Citrinin	54680783	1	1	1	4	4	5
Glabridin	124052	3	2	2	3	4	6
Mycocyclosin	59053147	3	1	1	3	5	6
2,3-Dehydro-UWM6	25195328	3	1	5	5	6	5
Prazepam	4890	4	1	2	3	4	6
(-)-Phaseollinisoflavan	162412	3	2	2	3	4	6
Phaseollidin	119268	3	2	4	5	6	4
Dibenzo[1,4]dioxin-2,3-dione	17036	3	2	1	5	6	5
Glycophymoline	5480	3	2	1	6	4	3
Flindersiachromone	441964	4	2	4	4	3	5
Arborine	63123	3	2	3	5	5	7
Methaqualone	6292	2	2	2	6	6	6
2-[3-Ethyl-5-(4-methoxyphenyl)-1H-pyrazol-4-yl]phenol	257428	2	1	2	8	5	5
Tutin	75729	1	1	1	8	4	4
(-)-Abscisic acid	643732	2	NA	0	9	7	NA
Alpha-beta-Dihydroresveratrol	185914	3	NA	2	11	5	6
3-(m-Aminophenyl)-2-(p-methoxyphenyl)acrylonitrile	79559	2	2	2	NA	NA	NA
(2-Butylbenzofuran-3-yl)(4-hydroxyphenyl)ketone	79569	3	NA	2	NA	3	6
Bergaptol	5280371	NA	2	1	12	6	5
Bergapten	2355	NA	2	1	8	5	6
Methylarbutin	80131	NA	2	NA	11	3	7
Abscisic acid	5280896	NA	NA	NA	11	5	NA
(+)-8'-Hydroxyabscisic acid	11954194	NA	NA	1	10	4	7
4-hydroxycoumarin	54682930	NA	NA	NA	NA	5	NA
Scopoletin	5280460	NA	NA	NA	NA	8	NA
Triamiphos	13943	NA	NA	NA	NA	6	NA

To visualize the binding profiles of the compounds across all six protein diseases, a graph can be constructed with the compounds on the x-axis and the number of binding locations within the protein coordinates on the y-axis. Each compound is represented by a bar, with the height of the bar indicating the number of binding locations within the protein coordinates for that compound. The graph provides an overview of the binding versatility of each compound across multiple protein targets associated with breast cancer and uterine fibroid, Graph 1.

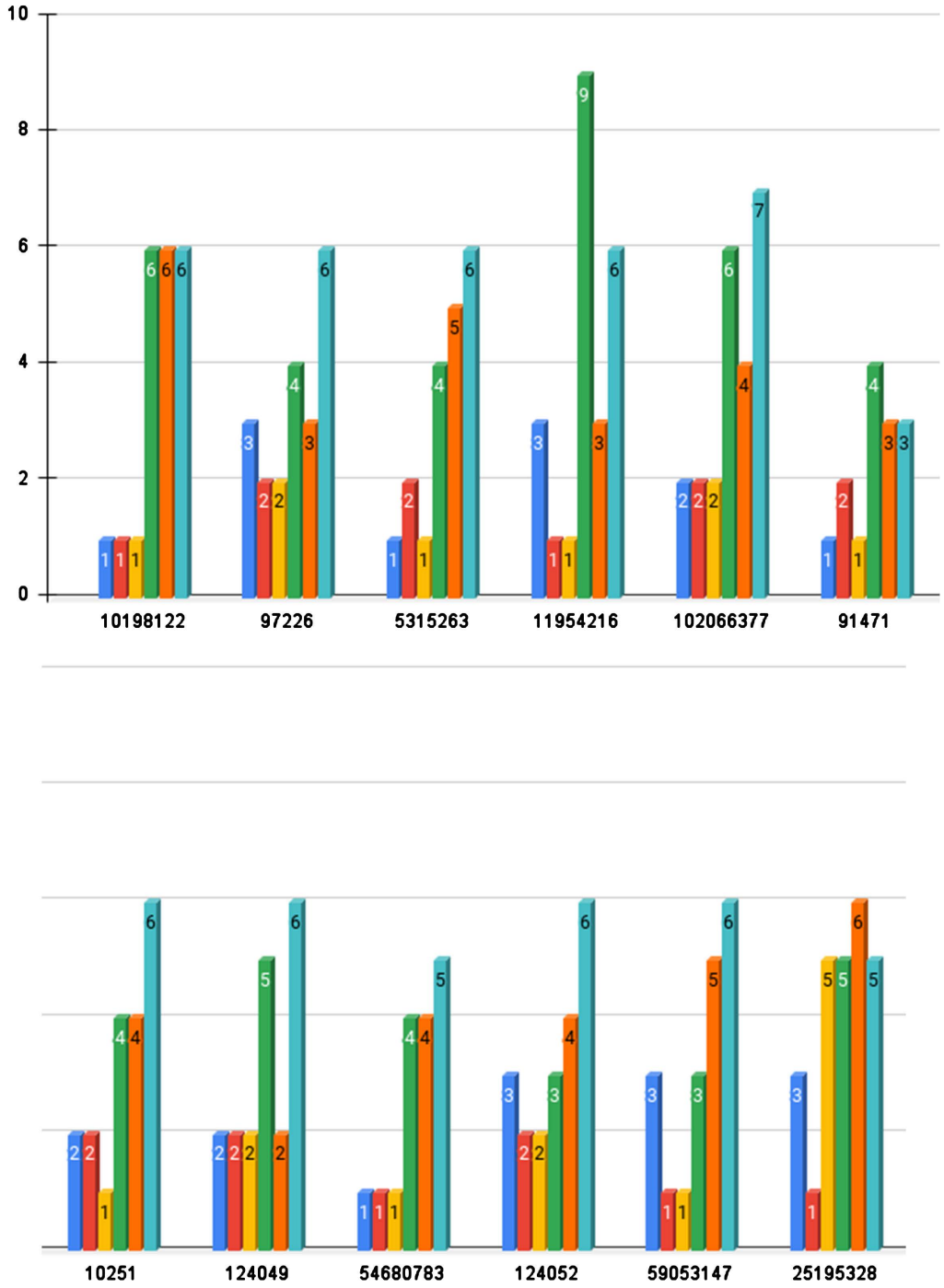

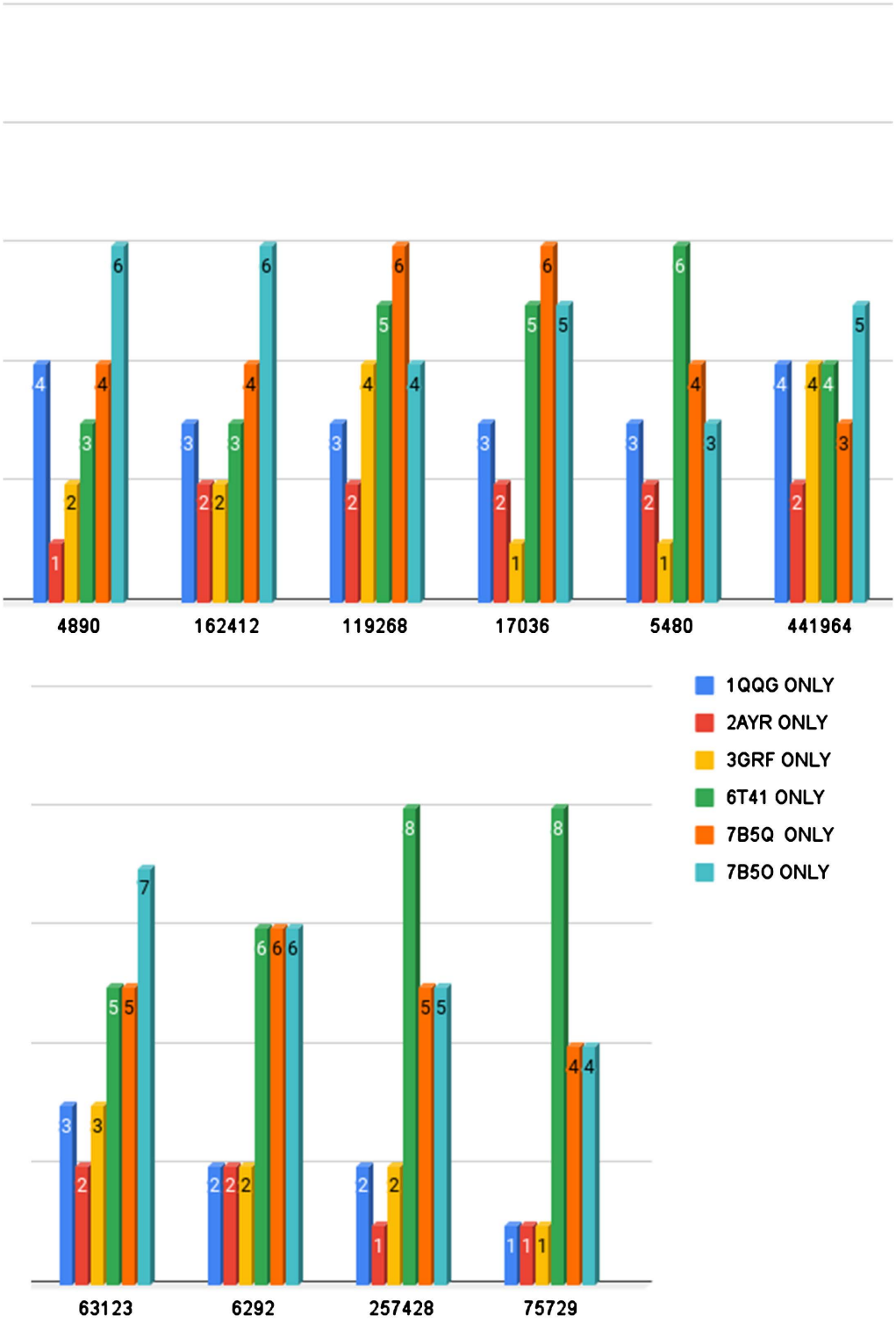

Graph 1. Show the graph for 22 compounds with the number of locations it's able to bind.

The comprehensive analysis of compound-protein interactions reveals distinct binding profiles across multiple protein targets implicated in breast cancer and uterine fibroid pathogenesis. Specifically, against the 1QQG protein, 26 compounds exhibit diverse binding patterns, with each compound displaying a va-

rying number of binding locations within the protein coordinates. Similarly, interactions with the 2AYR protein reveal comparable trends among 26 compounds, while interactions with the 3GRF, 6T41, 7B5Q, and 7B5O proteins demonstrate unique binding profiles for 29, 29, 33, and 28 compounds, respectively. These findings underscore the compound-specific nature of binding interactions and provide valuable insights for further exploration of therapeutic interventions targeting breast cancer and uterine fibroids in Graphs 2(a)-(f). Figures 12-17 show the one of the compounds of 10251 for each protein's locations within set coordinates.

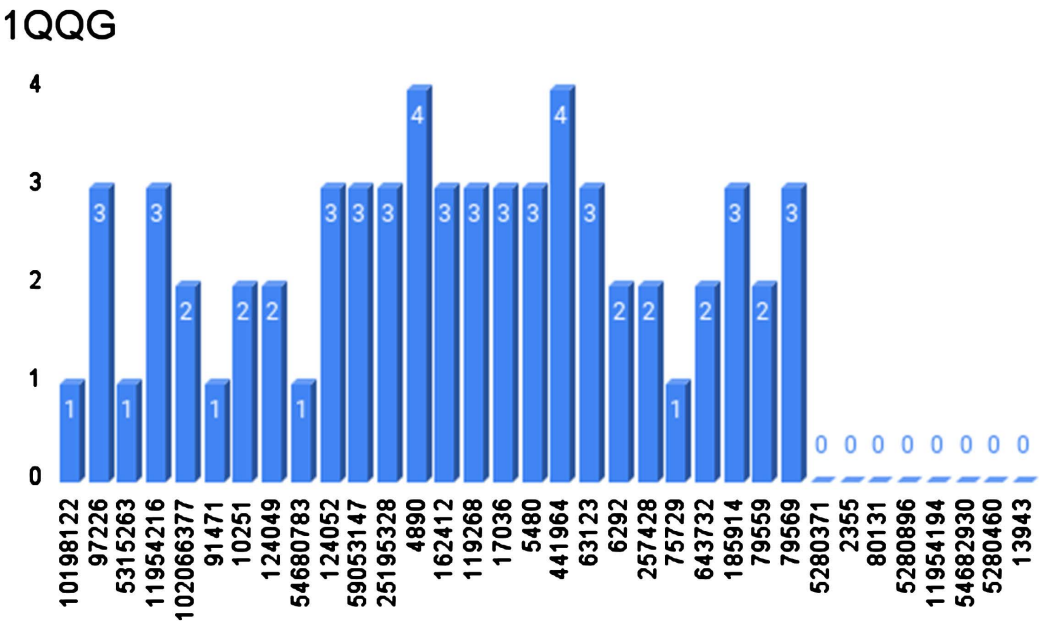

(a)

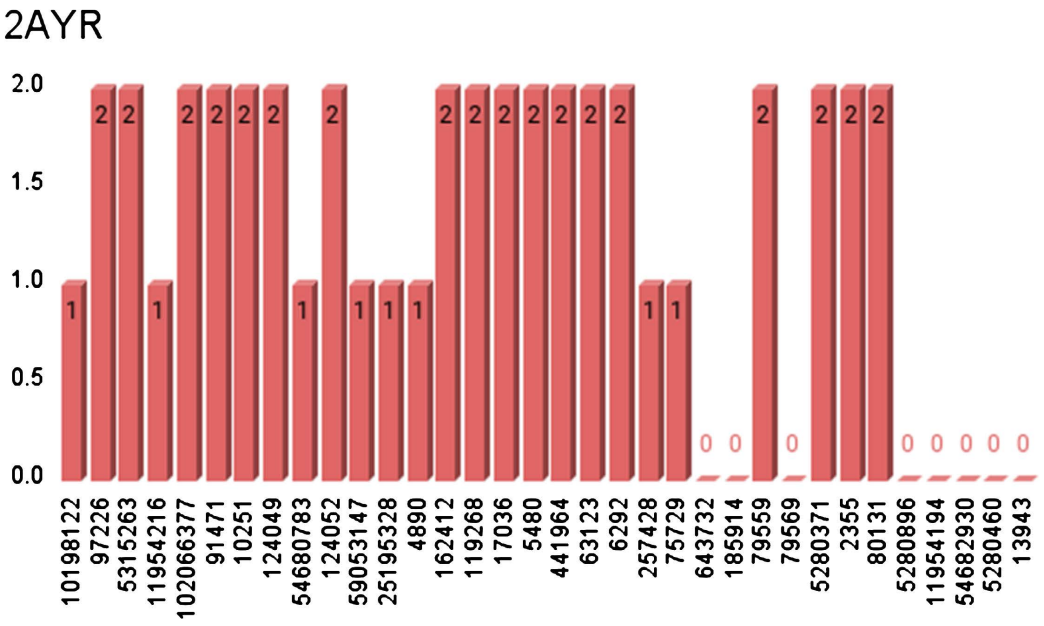

(b)

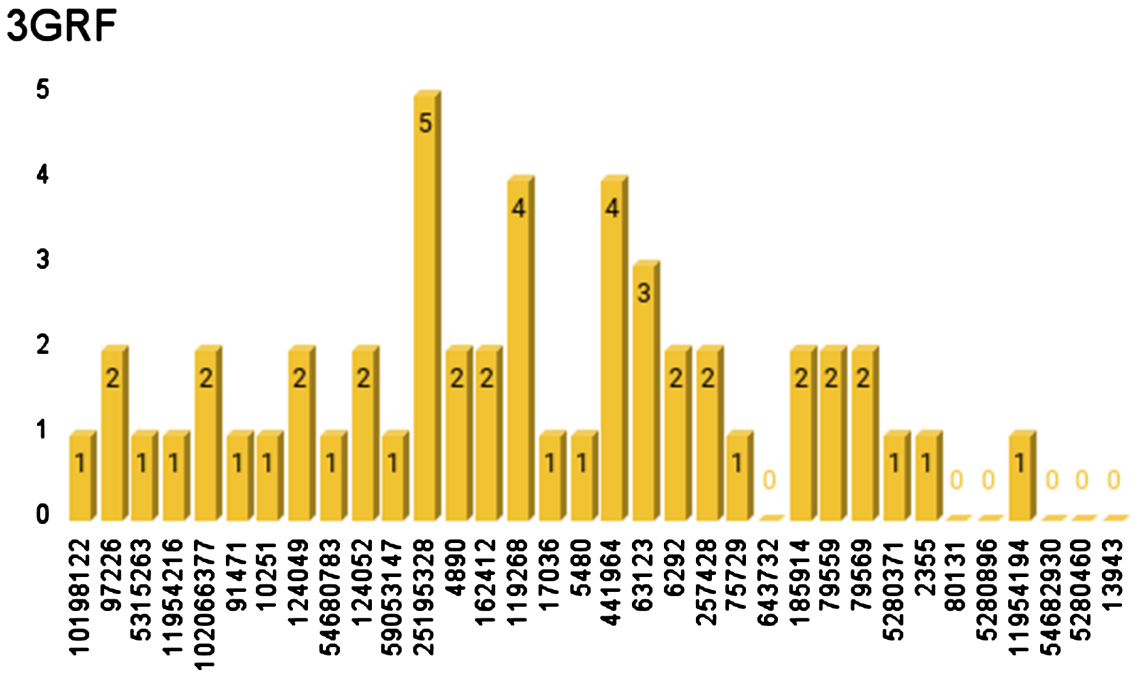
3GRF
0
1
2
3
4
5
1 2 1 1 2 1 1 2 1 2 1 5 2 2 4 1 1 4 3 2 2 1 0 2 2 2 1 1 0 0 1 0 0 0
10198122
97226
5315263
11954216
102066377
91471
10251
124049
54680783
124052
59053147
25195328
4890
162412
119268
17036
5480
441964
63123
6292
257428
75729
643732
185914
79559
79569
5280371
2355
80131
5280896
11954194
54682930
5280460
13943

(c)

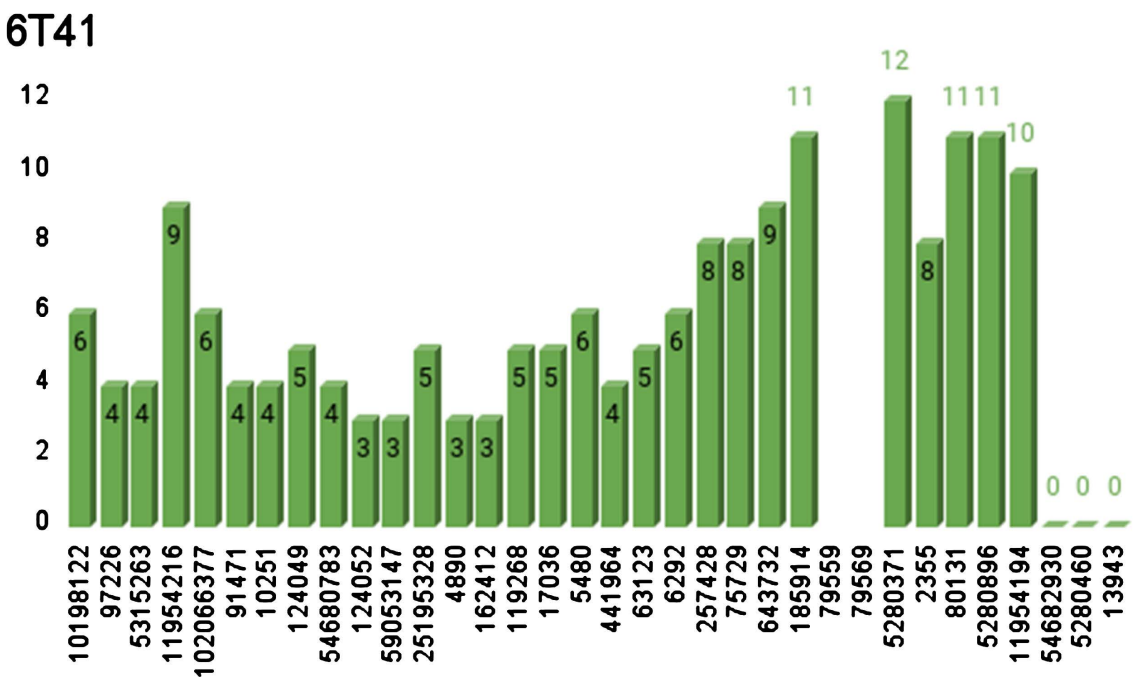
6T41
0
2
4
6
8
10
12
6 4 4 9 6 4 4 5 4 3 3 5 3 3 5 5 6 4 5 6 8 8 9 11 12 8 11 11 10 0 0 0
10198122
97226
5315263
11954216
102066377
91471
10251
124049
54680783
124052
59053147
25195328
4890
162412
119268
17036
5480
441964
63123
6292
257428
75729
643732
185914
79559
79569
5280371
2355
80131
5280896
11954194
54682930
5280460
13943

(d)

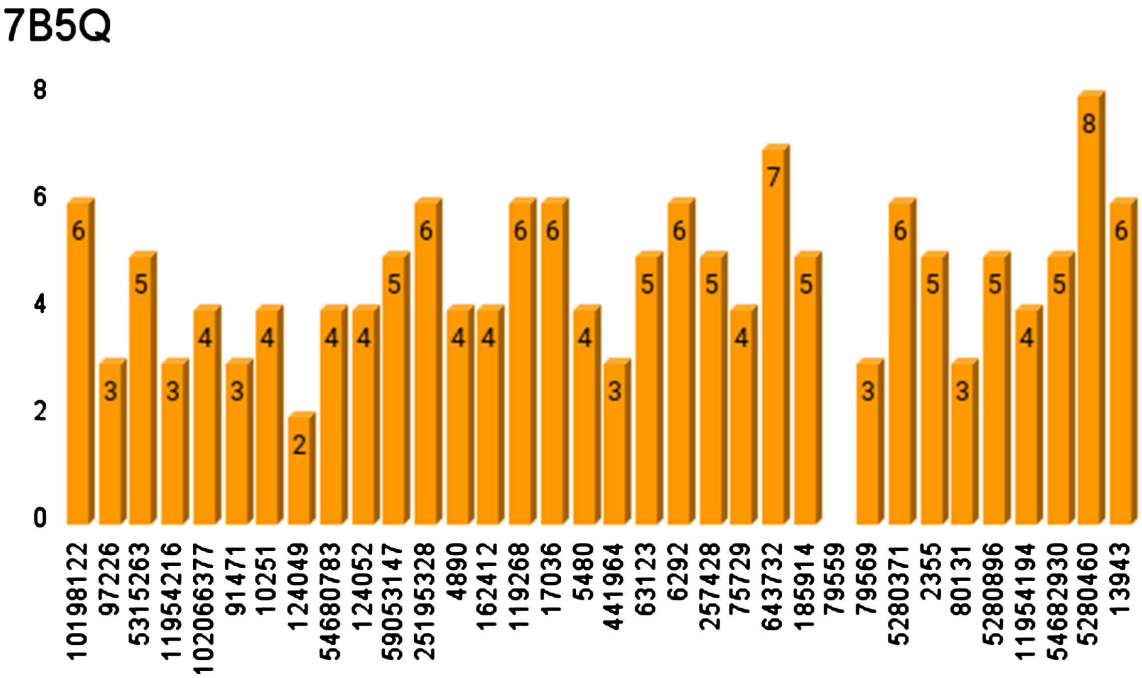

(e)

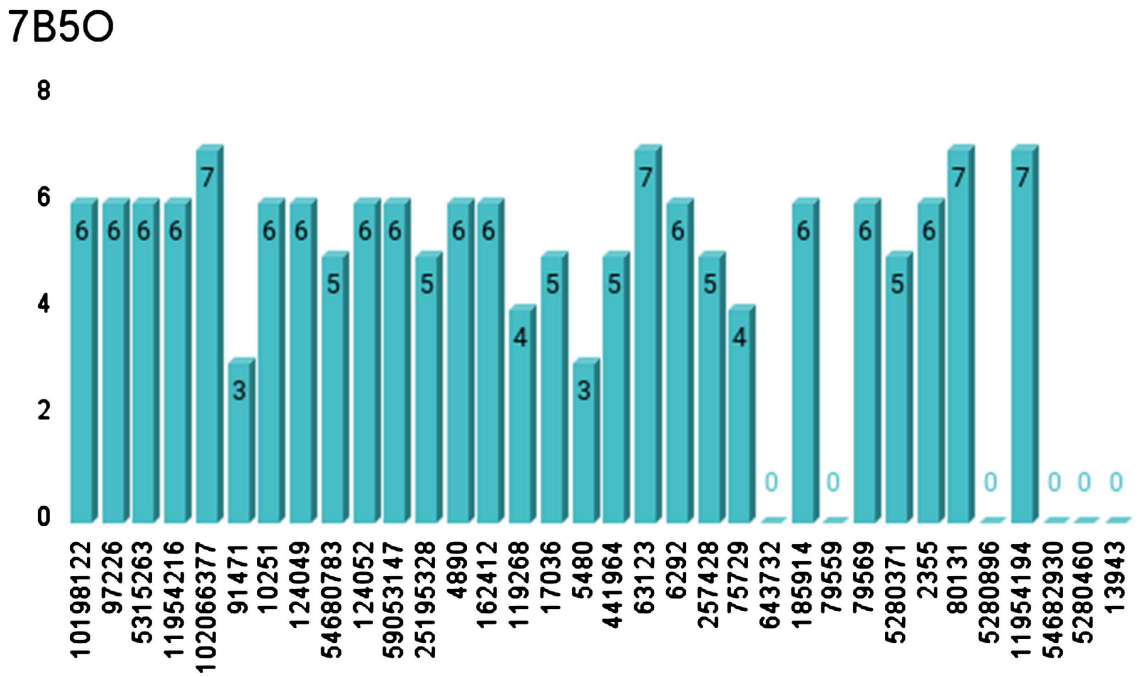

(f)

Graph 2. (a) Shows protein 1QQG's number of location binding for each compound; (b) Shows protein 2AYR's number of location binding for each compound; (c) Shows protein 3GRF's number of location binding for each compound; (d) Shows protein 6T41's number of location binding for each compound; (e) Shows protein 7B5Q's number of location binding for each compound; (f) Shows protein 7B5O's number of location binding for each compound.

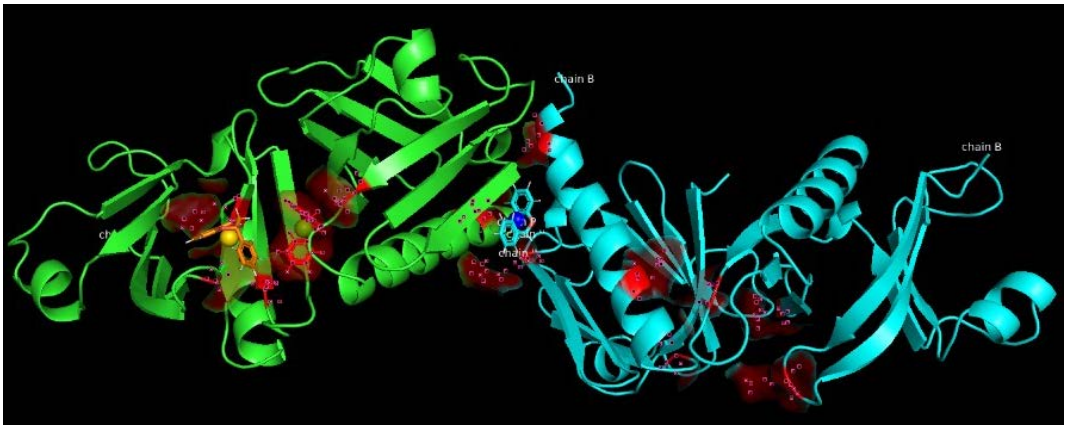

Figure 12. Shows compound 10251 location within set coordinate in 1QQG protein.

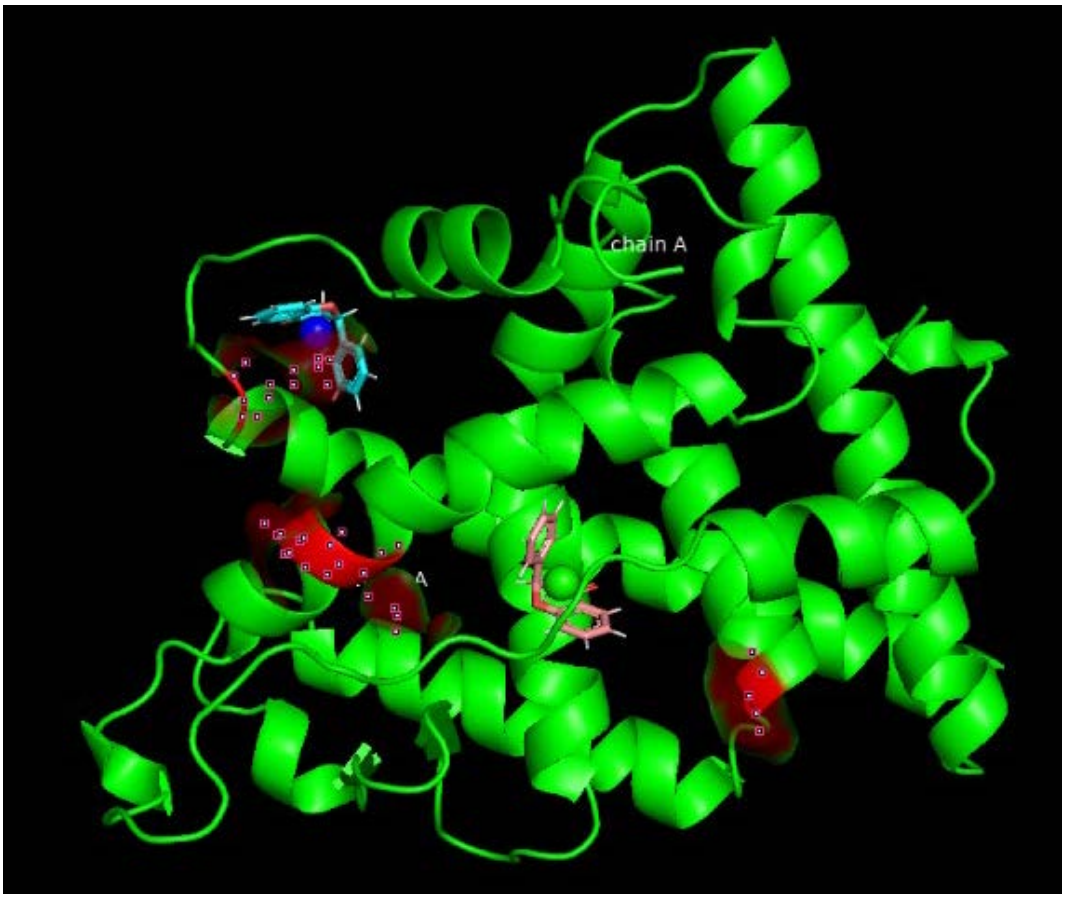

Figure 13. Shows compound 10251 location within set coordinate in 2AYR protein.

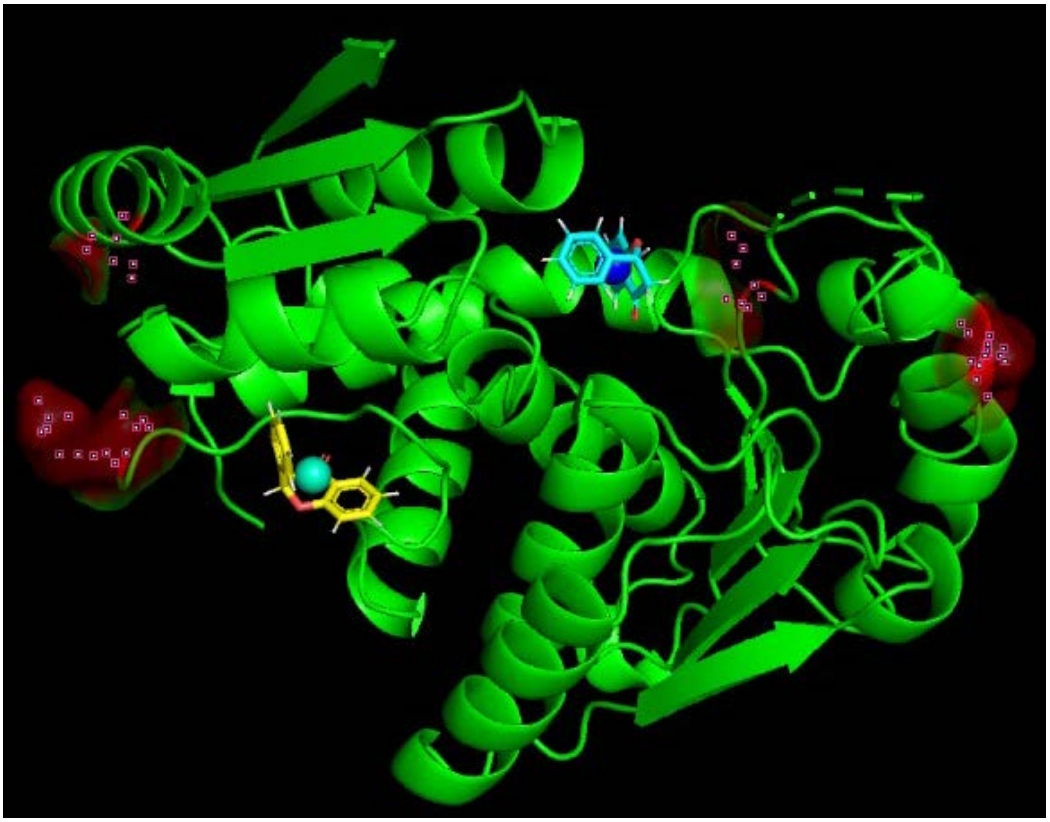

Figure 14. Shows compound 10251 location within set coordinate in 3GRF protein.

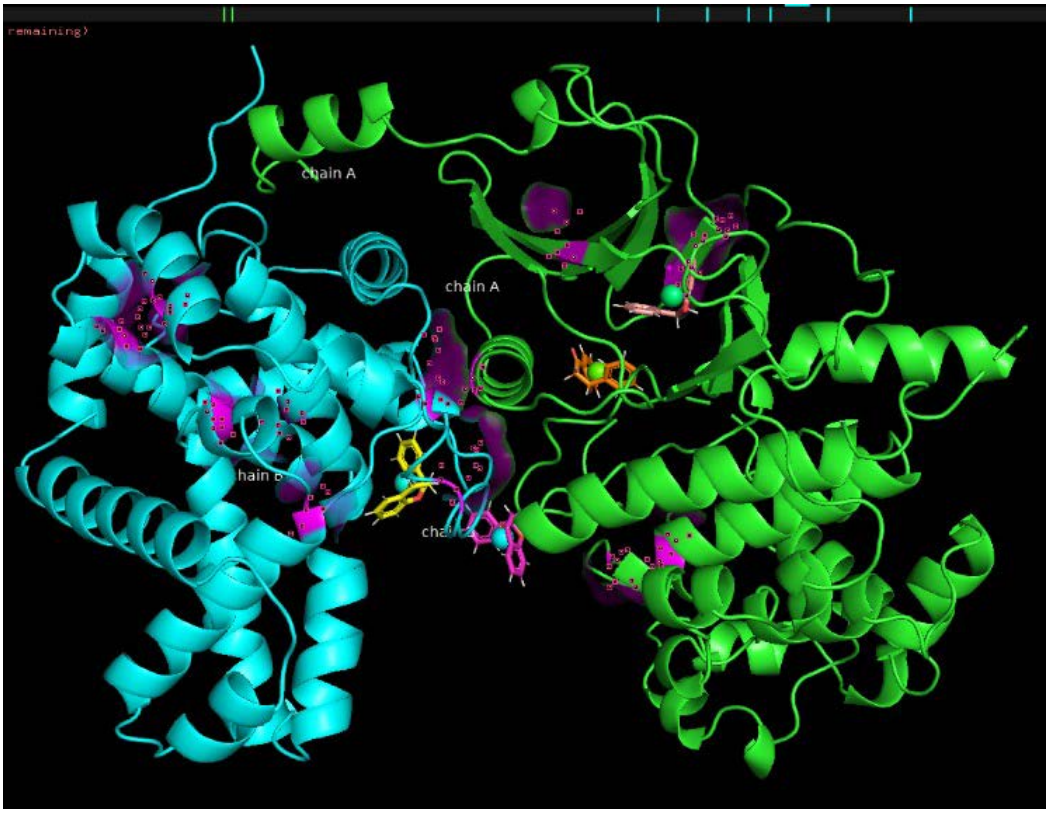

Figure 15. Shows compound 10251 location within set coordinate in 6T41 protein.

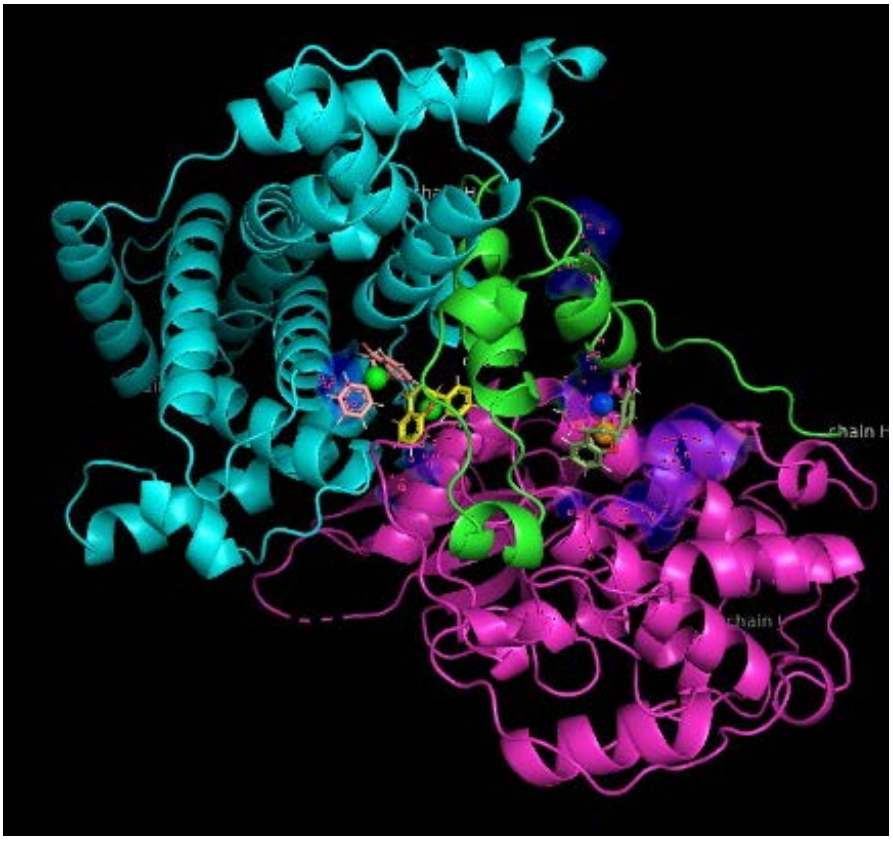

Figure 16. Shows compound 10251 location within set coordinate in 7B5Q protein.

Figure 17. Shows compound 10251 location within set coordinate in 7B5O protein.

The figure displays the distances between a specific compound and the amino acids of proteins associated with breast cancer and uterine fibroid pathogenesis. Specifically, it illustrates the distances to amino acids of proteins 1QQG, 7B5Q, and 7B5O, representing breast cancer-related proteins, as well as proteins 2AYR, 3GRF, and 6T41, which are associated with uterine fibroid disease. These distances serve as indicators of the successful rate of binding energy for the compound towards each protein disease. Variations in distance highlight the differing degrees of interaction between the compound and the amino acids within each protein structure. Shorter distances suggest stronger binding interactions, indicating a higher potential for therapeutic efficacy in reducing the propensity for breast cancer and uterine fibroid development. Conversely, longer distances may signify weaker binding interactions, suggesting a need for further investigation or optimization of the compound's efficacy.

By analyzing the distances to amino acids in the proteins relevant to both breast cancer and uterine fibroids, this table and 4 figures for each proteins provides valuable insights into the compound's potential effectiveness in targeting these diseases. This information aids in the identification and prioritization of compounds for further preclinical and clinical studies aimed at mitigating the progression of breast cancer and uterine fibroids, **Figures 18-23**.

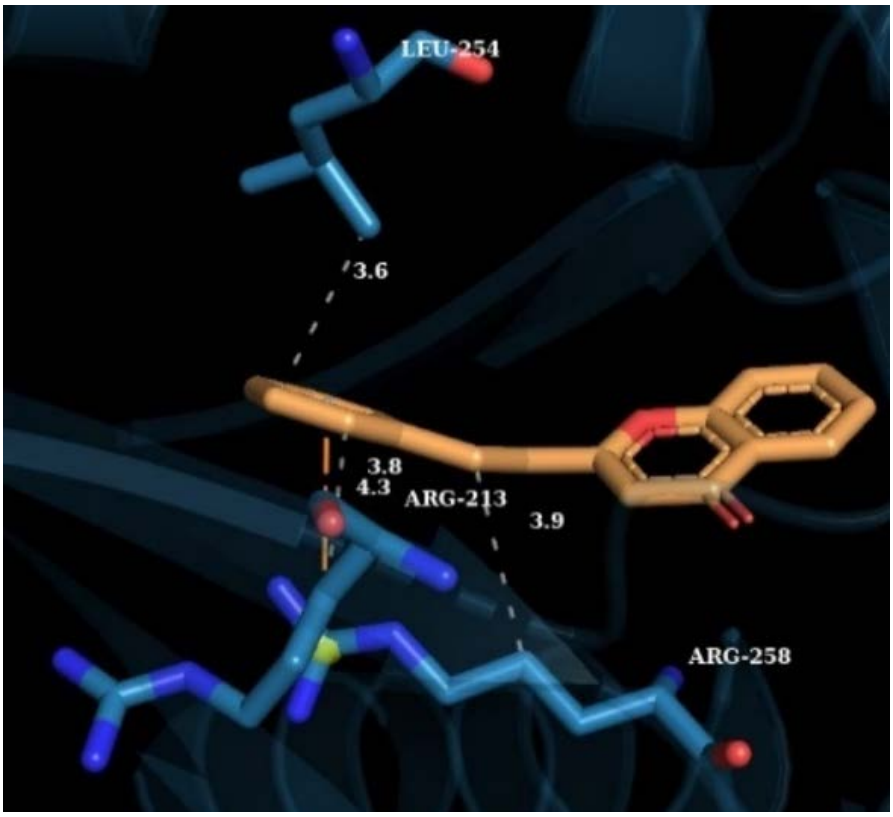

(a)

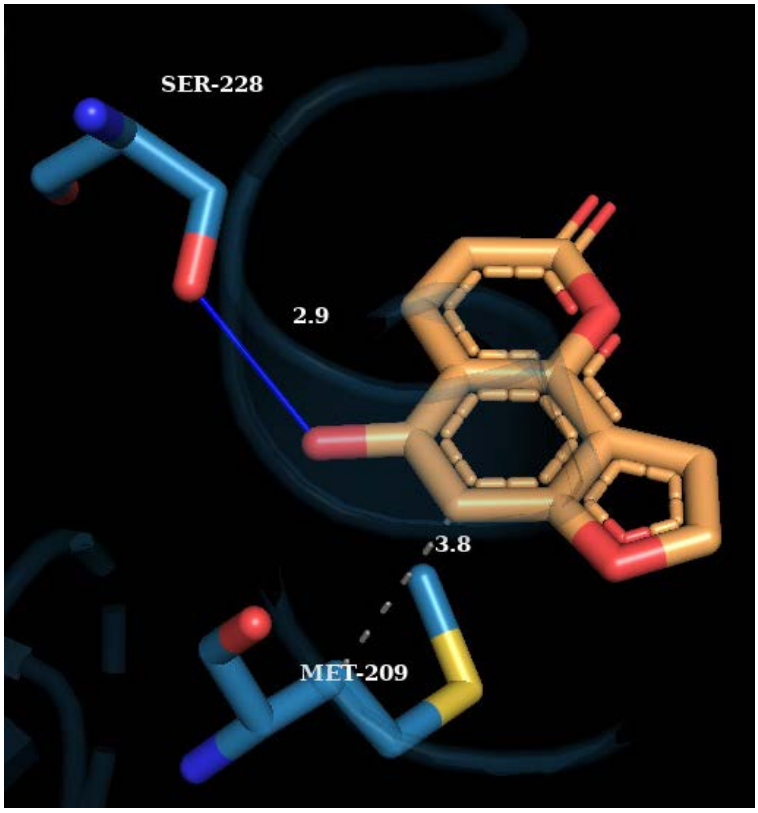

(b)

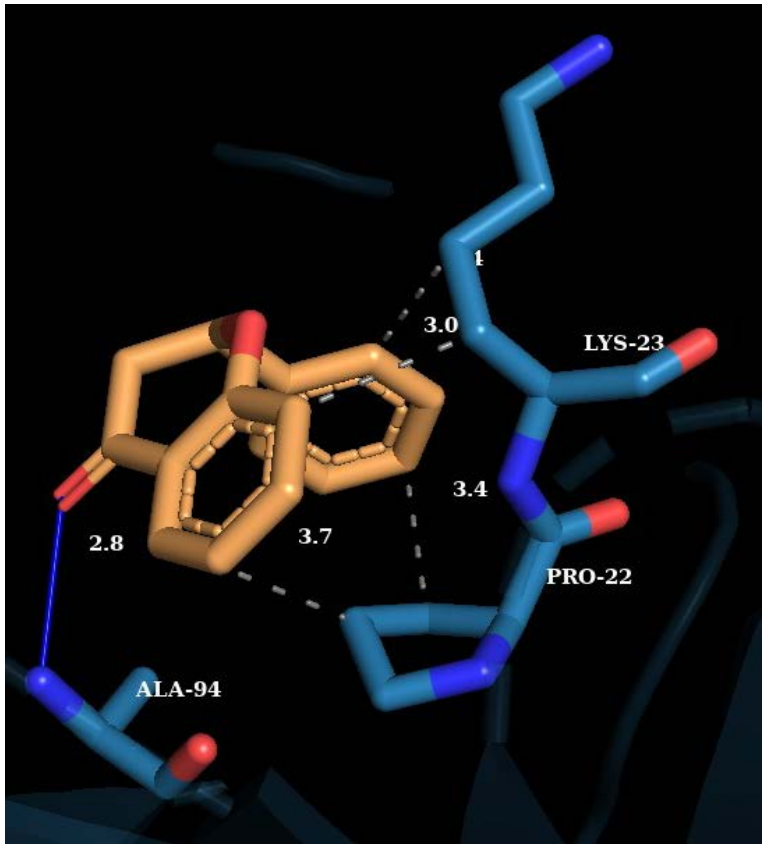

(c)

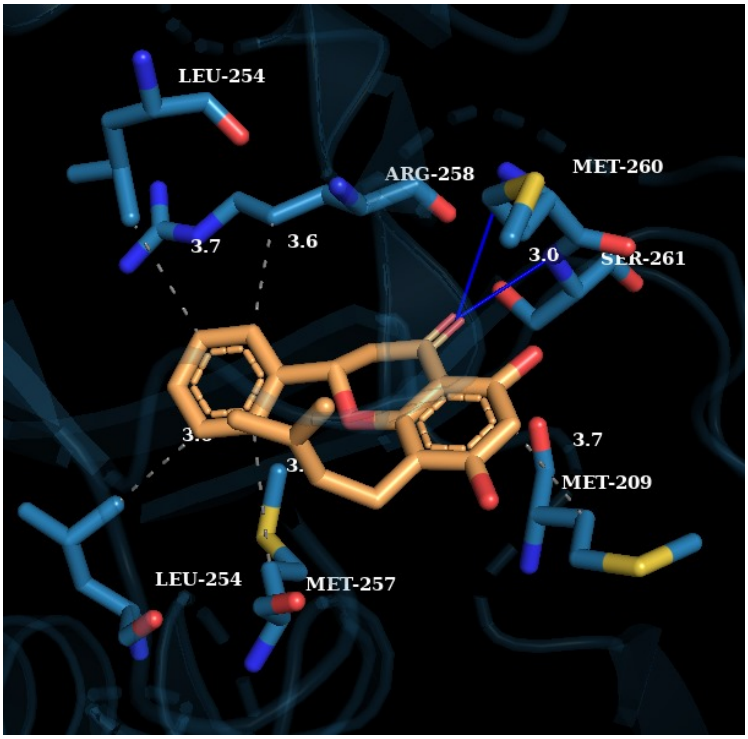

(d)

Figure 18. (a) Shows protein 1QQG interactions and distance from compound 441964 amino acids with the nearest distances of 3.6; (b) Shows protein 1QQG interactions and distance from compound 10198122 amino acids with the nearest distances of 2.9; (c) Shows protein 1QQG interactions and distance from compound 10251 amino acids with the nearest distances of 2.8; (d) Shows protein 1QQG interactions and distance from compound 124049 amino acids with the nearest distances of 3.0.

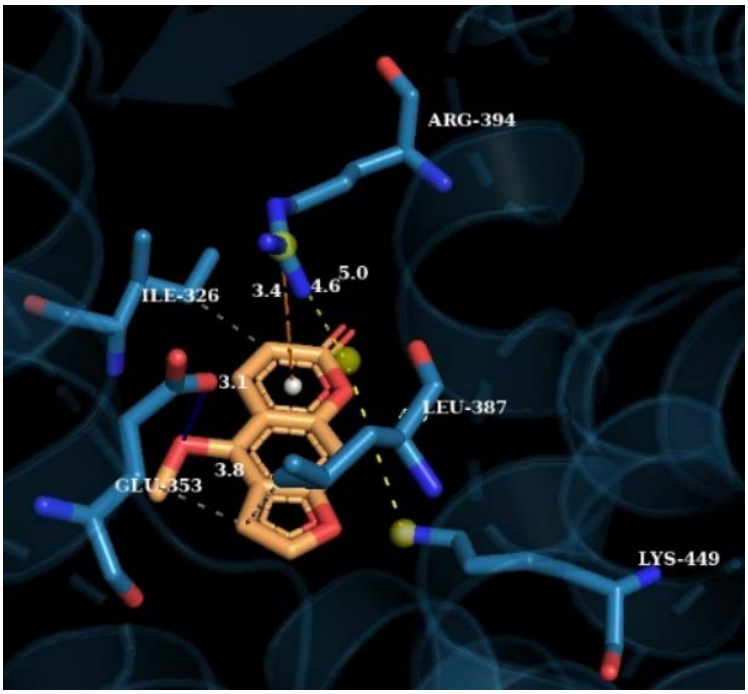

(a)

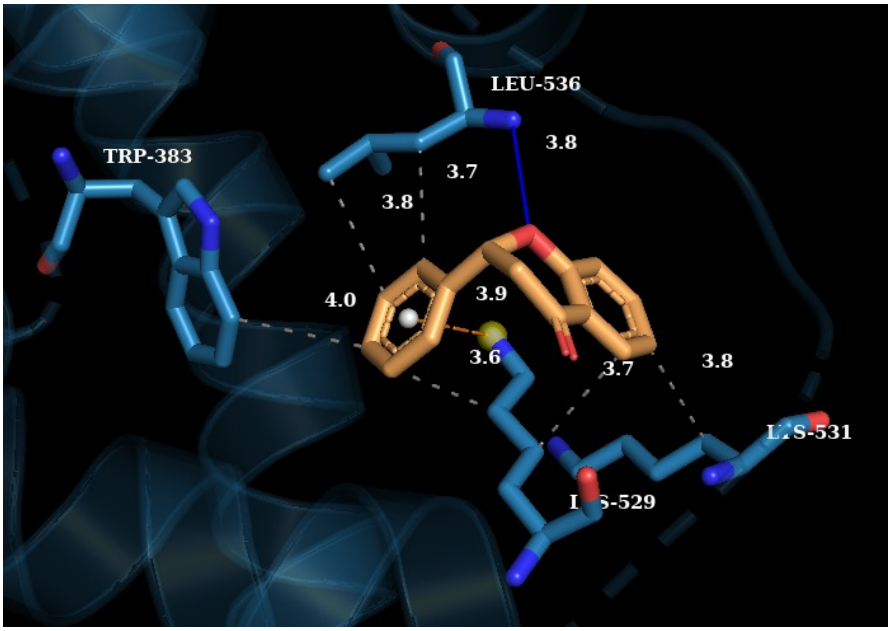
LEU-536
TRP-383
3.8
3.7
3.8
4.0
3.9
3.6
3.7
3.8
LYS-531
LYS-529

(b)

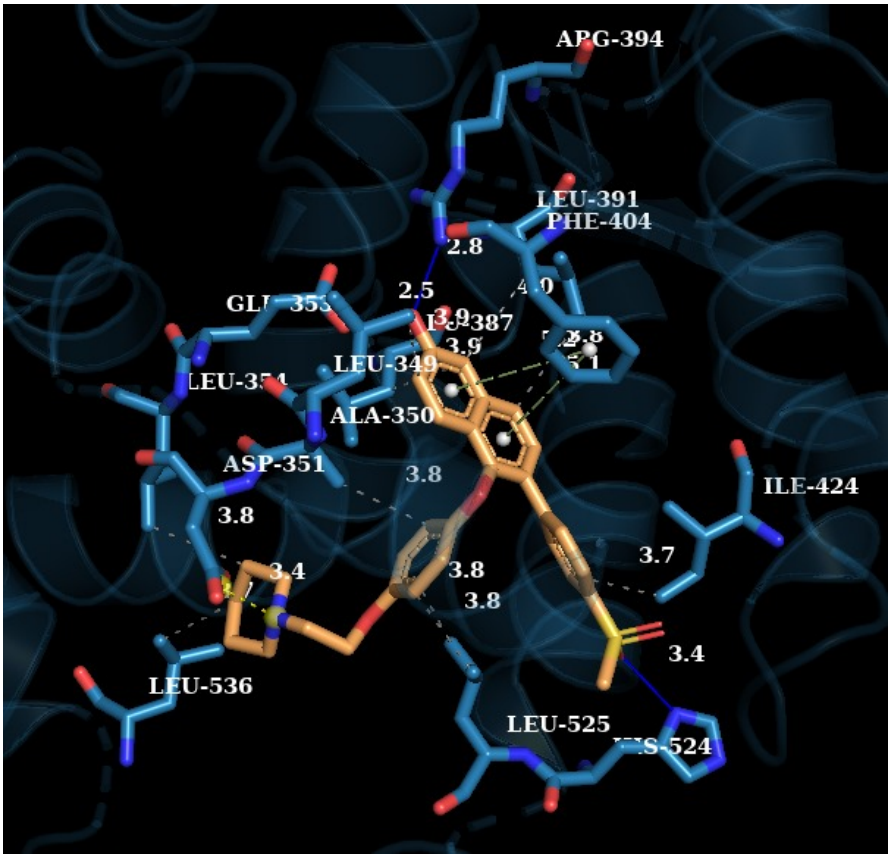
APG-394
LEU-391
PHE-404
2.8
2.5
GLU-353
LEU-349
LEU-354
ALA-350
ASP-351
3.8
3.8
3.4
3.8
3.8
3.7
ILE-424
3.4
LEU-536
LEU-525
HIS-524

(c)

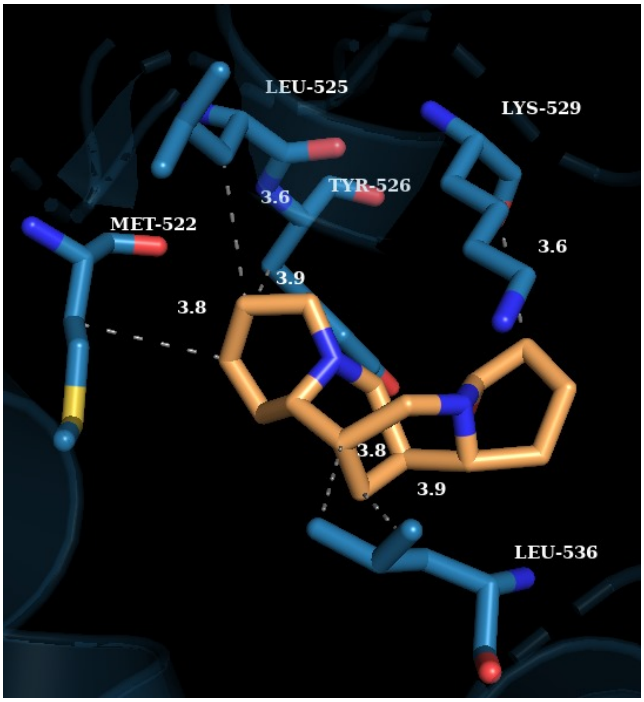

(d)

Figure 19. (a) Shows protein 2AYR interactions and distance from compound 2355 amino acids with the nearest distances of 3.1; (b) Shows protein 2AYR interactions and distance from compound 10251 amino acids with the nearest distances of 3.6; (c) Shows protein 2AYR interactions and distance from compound 80131 amino acids with the nearest distances of 2.5; (d) Shows protein 2AYR interactions and distance from compound 91471 amino acids with the nearest distances of 3.6

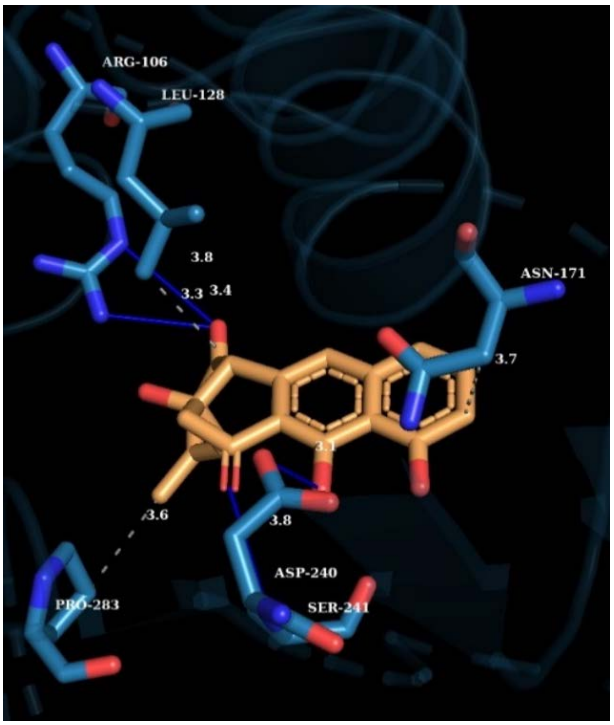

(a)

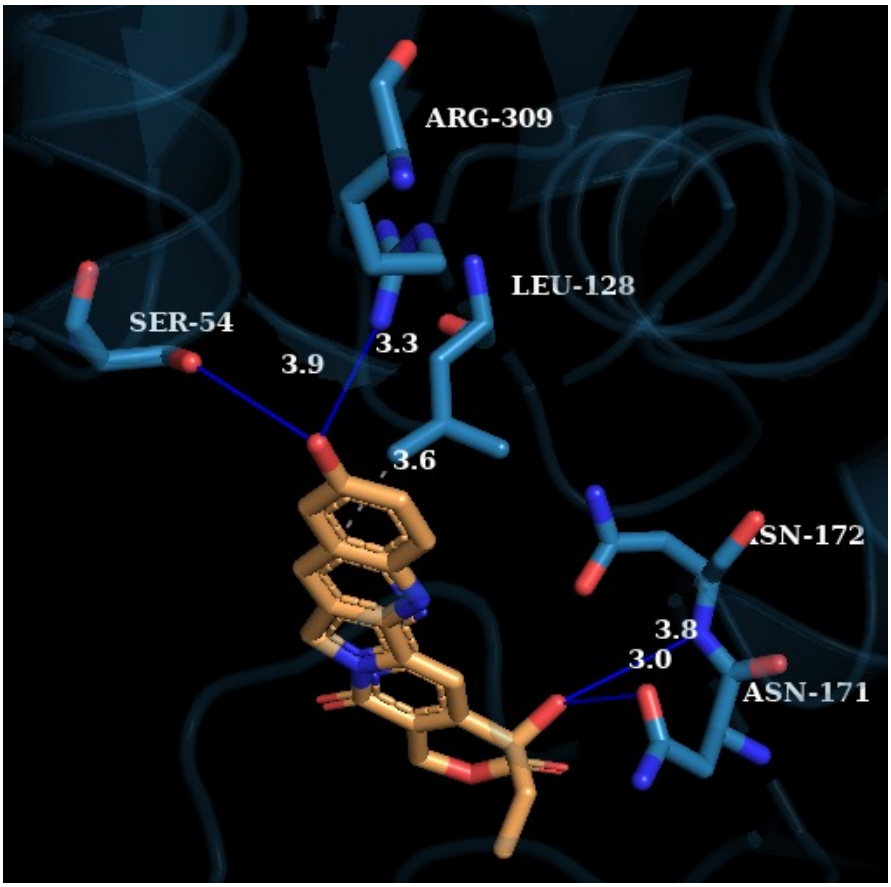
ARG-309
LEU-128
SER-54
3.3
3.9
3.6
SN-172
3.8
3.0
ASN-171

(b)

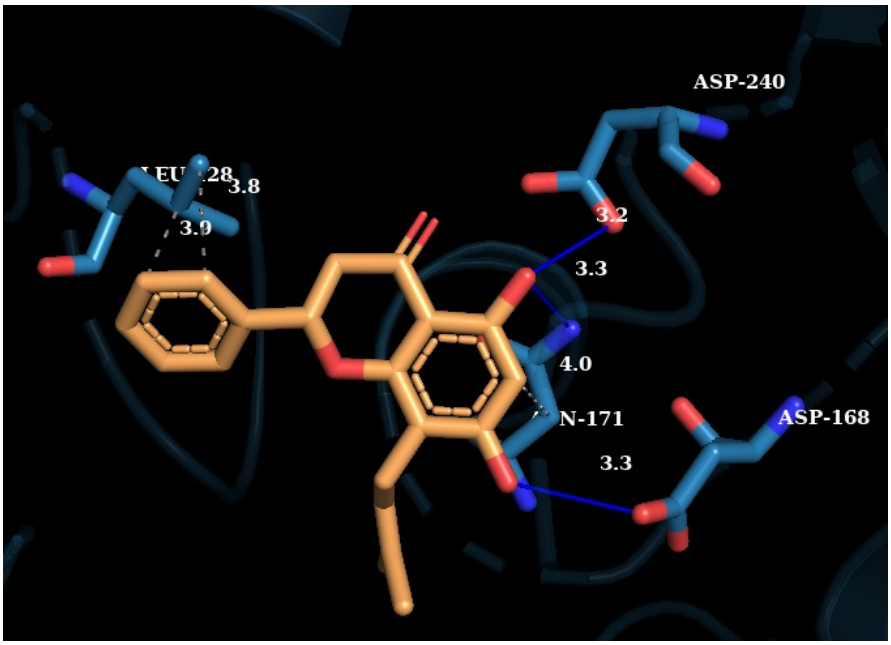
ASP-240
28
3.8
3.9
3.2
3.3
4.0
N-171
ASP-168
3.3

(c)

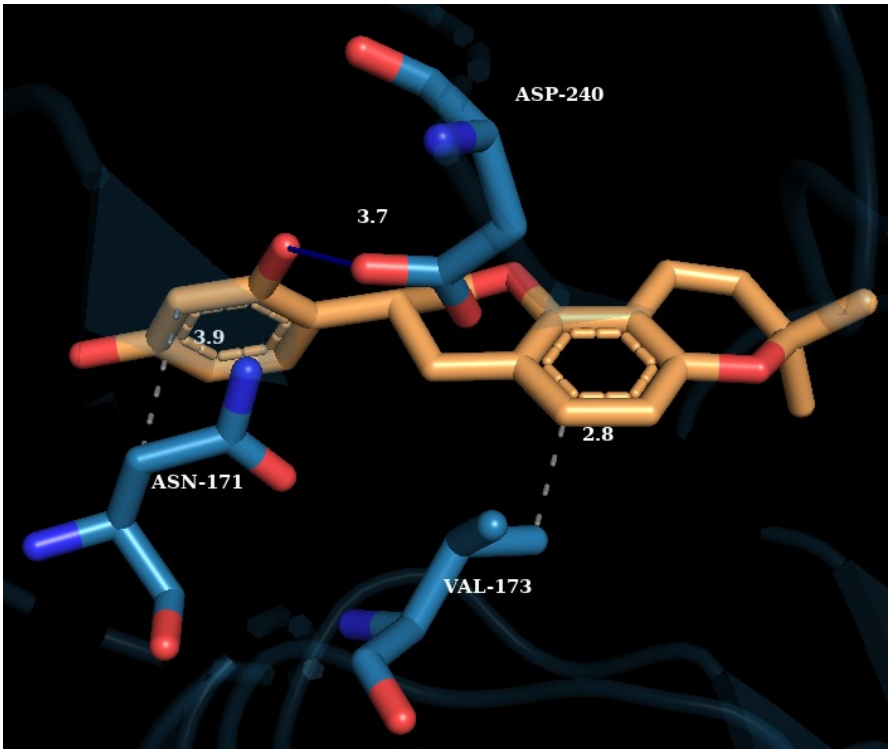

(d)

Figure 20. (a) Shows protein 3GRF interactions and distance from compound 25195328 amino acids with the nearest distances of 3.3; (b) Shows protein 3GRF interactions and distance from compound 97226 amino acids with the nearest distances of 3.0; (c) Shows protein 3GRF interactions and distance from compound 124049 amino acids with the nearest distances of 3.2; (d) Shows protein 3GRF interactions and distance from compound 124052 amino acids with the nearest distances of 2.8

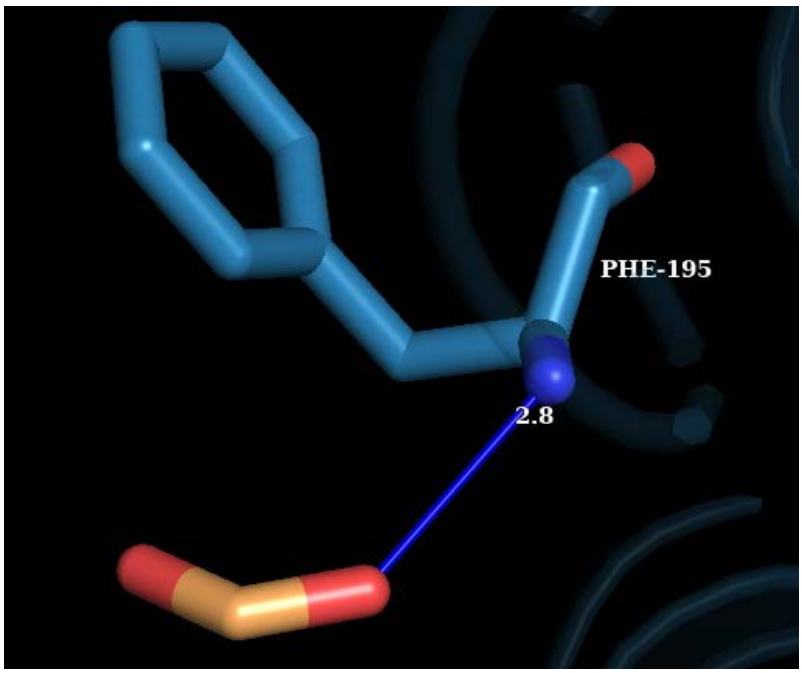

(a)

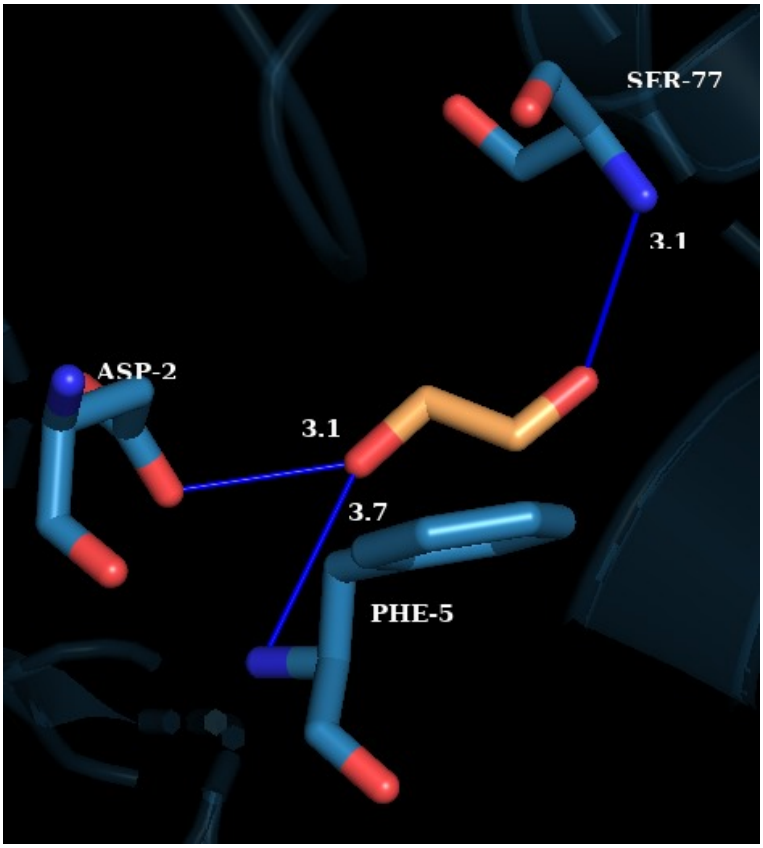

(b)

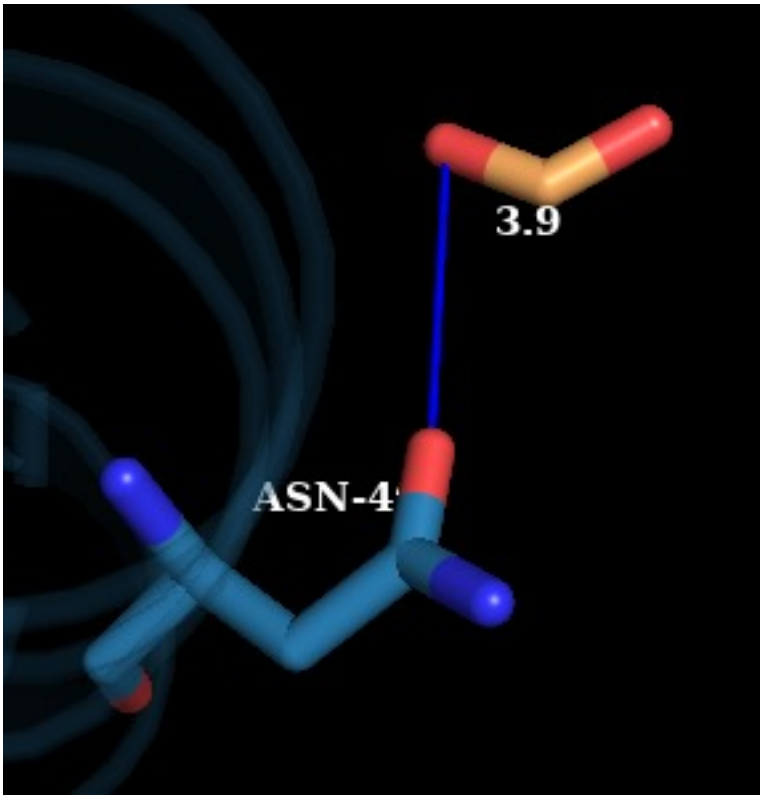

(c)

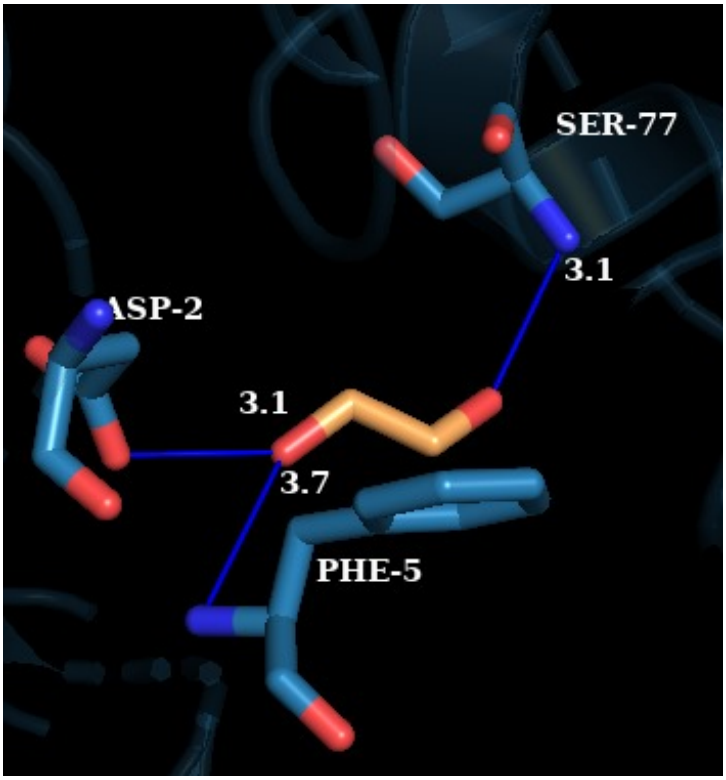

(d)

Figure 21. (a) Shows protein 6T41 interactions and distance from compound 5280371 amino acids with the nearest distances of 2.8; (b) Shows protein 6T41 interactions and distance from compound 4890 amino acids with the nearest distances of 3.1; (c) Shows protein 6T41 interactions and distance from compound 5480 amino acids with the nearest distances of 3.9; (d) Shows protein 6T41 interactions and distance from compound 6292 amino acids with the nearest distances of 3.1.

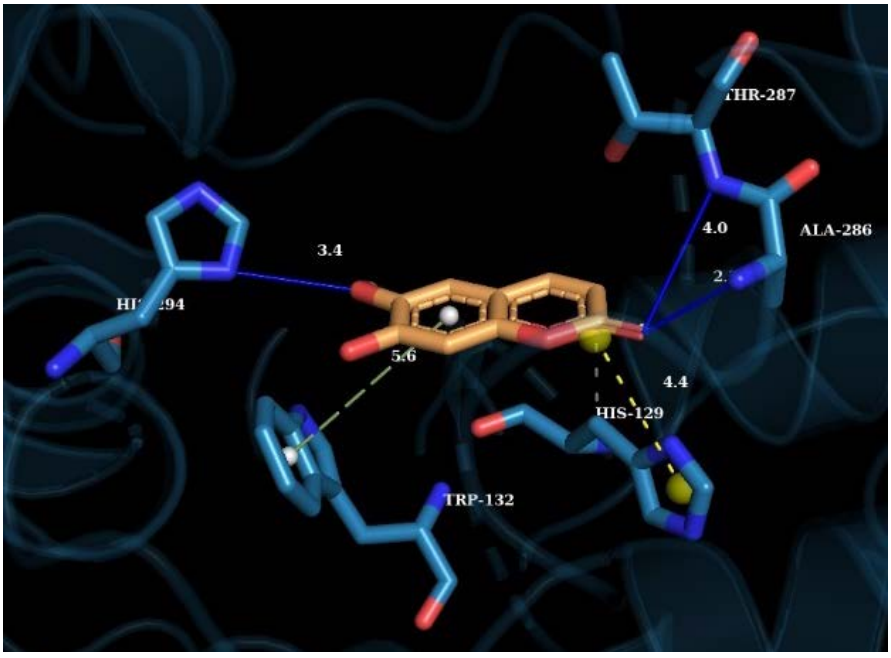

(a)

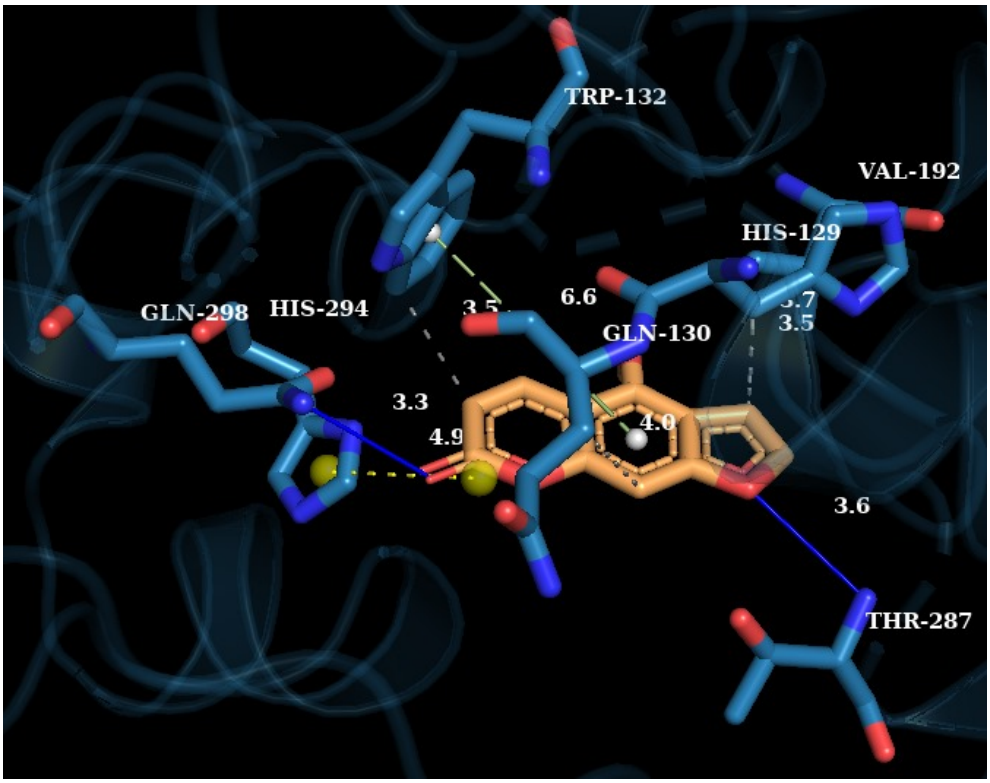
TRP-132
VAL-192
HIS-129
GLN-298
HIS-294
6.6
GLN-130
3.7
3.5
3.3
4.9
4.0
3.6
THR-287

(b)

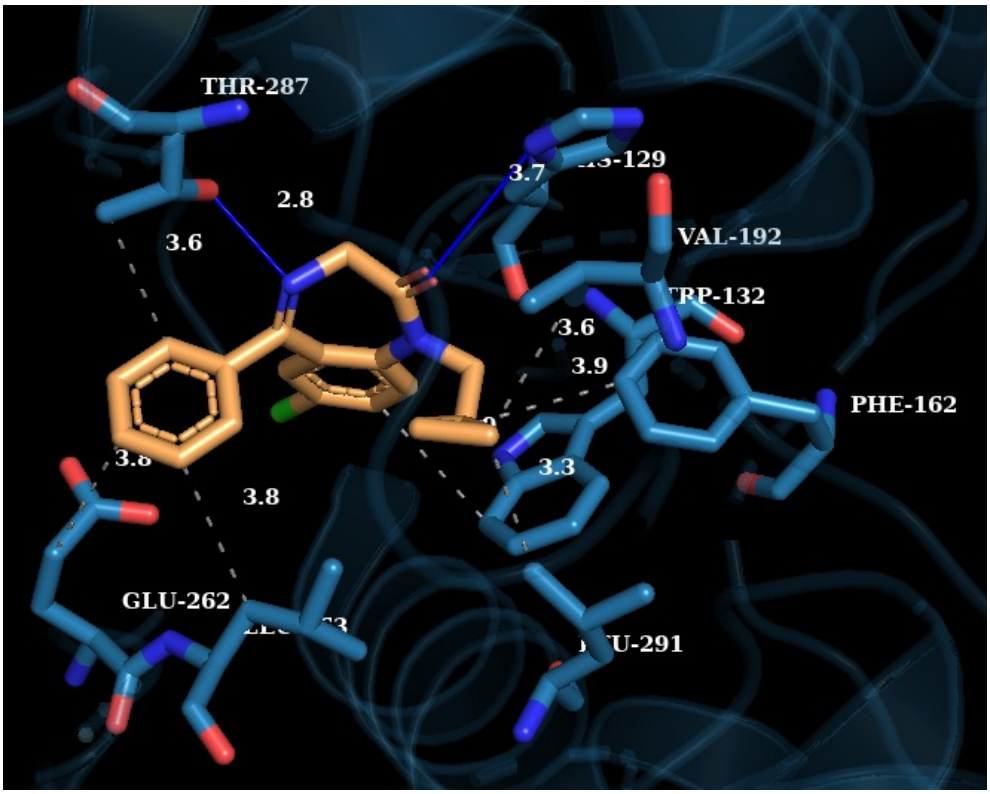
THR-287
3.7
2.8
3.6
VAL-192
3.6
3.9
PHE-162
3.3
3.8
GLU-262

(c)

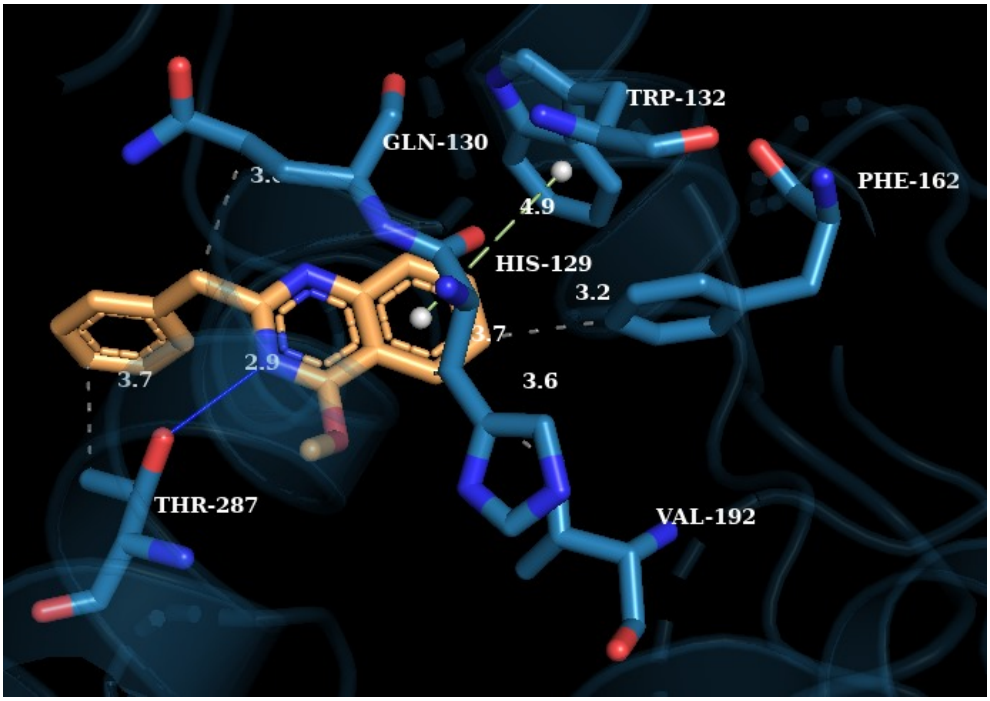

(d)

Figure 22. (a). Shows protein 7B5Q interactions and distance from compound 5280460 amino acids with the nearest distances of 2.0; (b) Shows protein 7B5Q interactions and distance from compound 2355 amino acids with the nearest distances of 3.3; (c) Shows protein 7B5Q interactions and distance from compound 4890 amino acids with the nearest distances of 2.8; (d) Shows protein 7B5Q interactions and distance from compound 5480 amino acids with the nearest distances of 2.9.

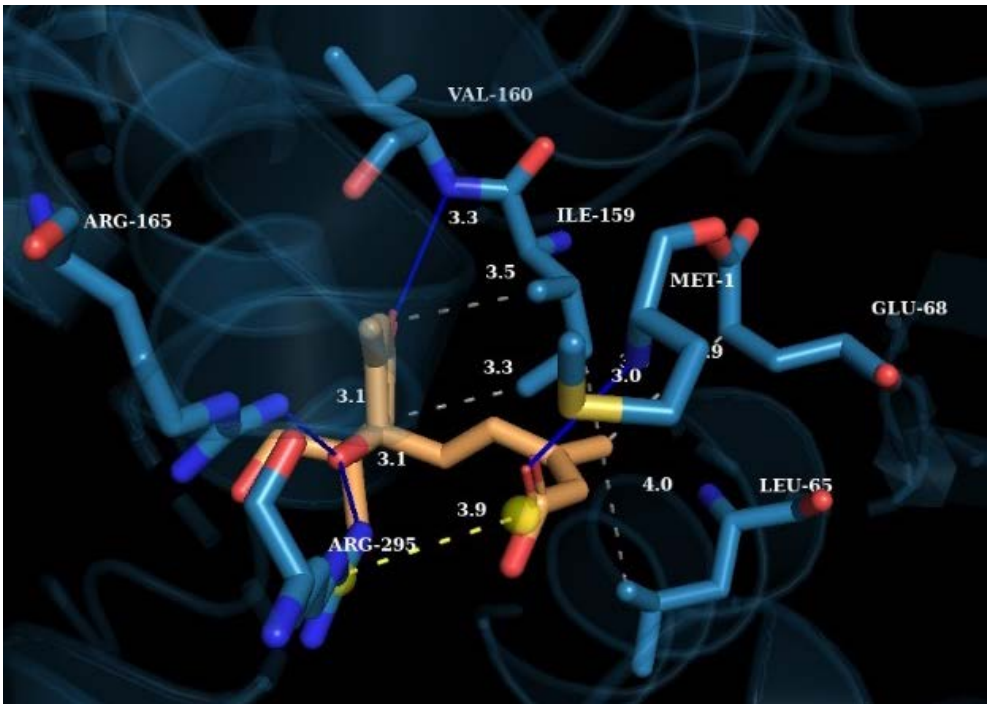

(a)

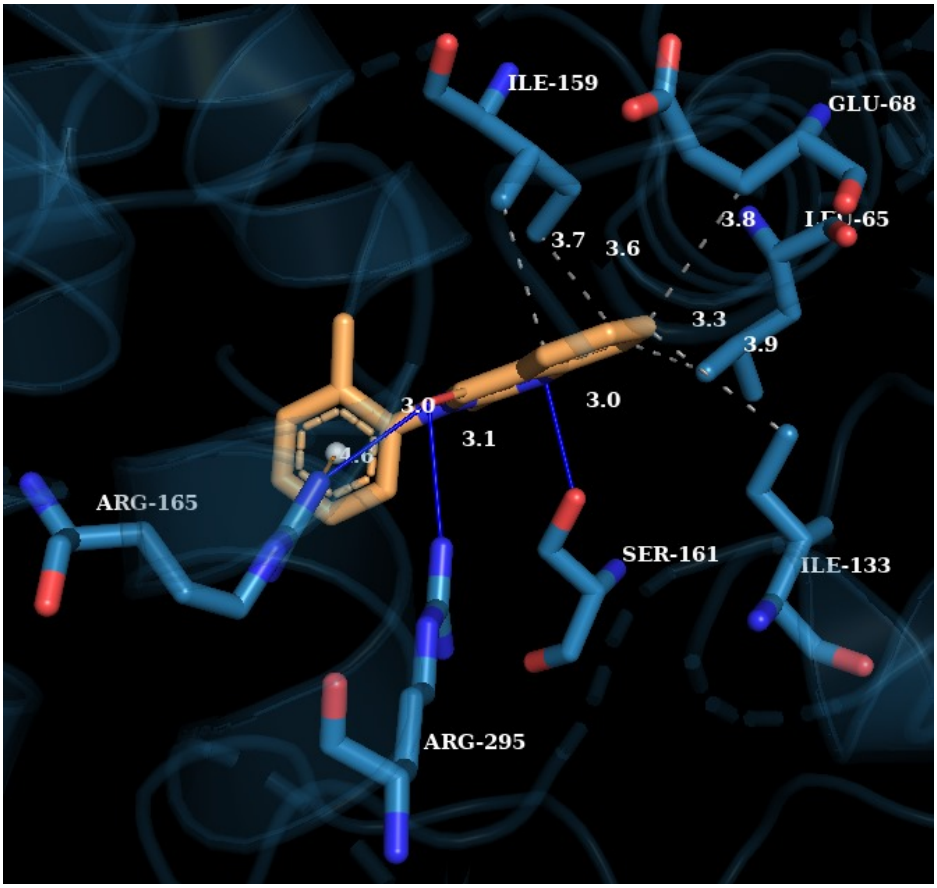
ILE-159
GLU-68
3.8
3.7
3.6
3.3
3.9
3.0
3.0
3.1
ARG-165
SER-161
ILE-133
ARG-295

(b)

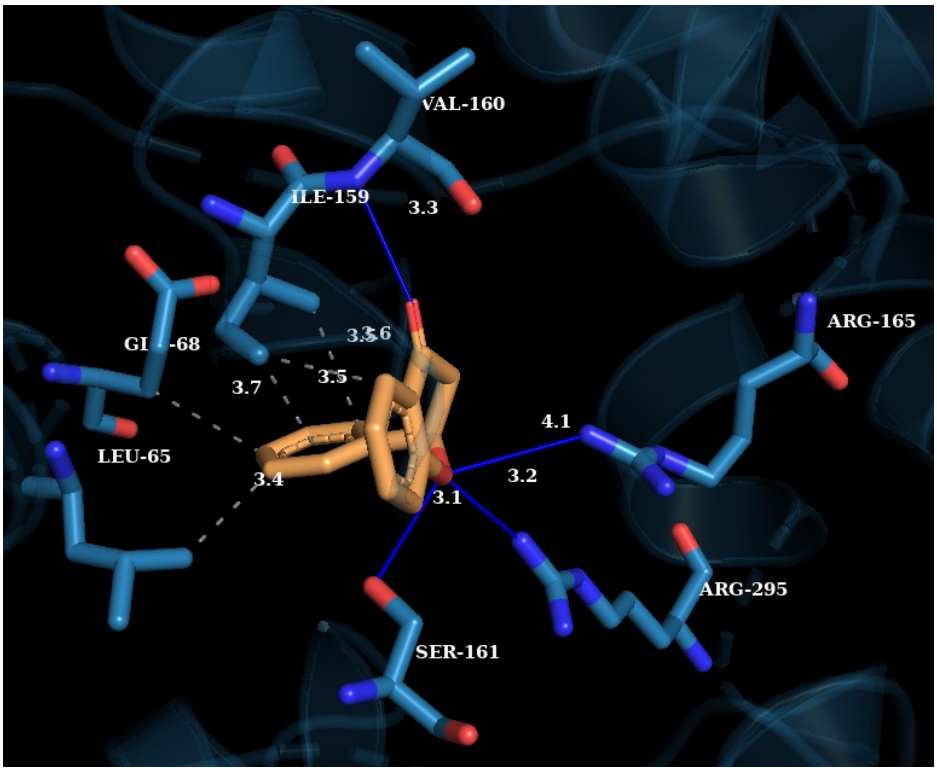
VAL-160
ILE-159
3.3
3.6
3.7
3.5
4.1
3.2
3.4
3.1
ARG-165
LEU-65
ARG-295
SER-161

(c)

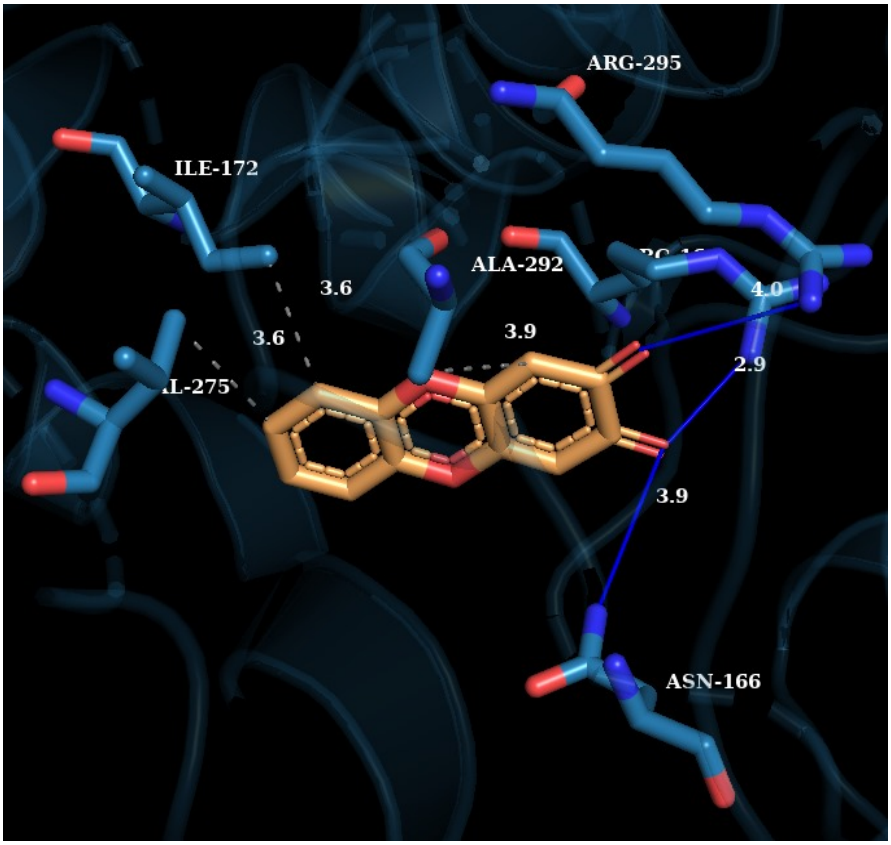

(d)

Figure 23. (a) Shows protein 7B5O interactions and distance from compound 11954194 amino acids with the nearest distances of 3.0; (b) Shows protein 7B5O interactions and distance from compound 6292 amino acids with the nearest distances of 3.0; (c) Shows protein 7B5O interactions and distance from compound 10251 amino acids with the nearest distances of 3.1; (d) Shows protein 7B5O interactions and distance from compound 17036 amino acids with the nearest distances of 2.9.

4. Discussion

The compounds that have been found in the LifeGreen™ product provide various benefits towards human health, breast cancers and uterine fibroid. Isobergaptol is a compound found in certain plants, particularly in essential oils. It has been studied for its potential anti-inflammatory and antimicrobial properties, which could contribute to improved immune function and wound healing. Some research suggests that Isobergaptol may also have antioxidant properties, helping to neutralize harmful free radicals in the body and reduce oxidative stress, which is associated with various chronic diseases. 10-Hydroxycamptothecin is a naturally occurring compound found in the Camptotheca acuminata tree. It is a derivative of camptothecin, a well-known anticancer agent. Studies have shown that 10-Hydroxycamptothecin exhibits potent antitumor activity by inhibiting the enzyme topoisomerase I, which is involved in DNA replication. This action can prevent cancer cells from proliferating and induce apoptosis (programmed cell death) in cancer cells. Camptothecin and related analogs have shown prom-

ise as anticancer agents, which could lead to the death of tumor cells by targeting the nuclear enzyme, topoisomerase I, and inhibiting the relegation of the cleaved DNA strand. One of the camptothecin analogs, hydroxycamptothecin (HCPT), a plant alkaloid derived from Camptotheca acuminata, has demonstrated strong antitumor activity against gastric, lung, ovarian, breast, and pancreatic carcinomas [23]. 10-hydroxycamptothecin (10-HCPT) is an important class of antitumor agent, it inhibits the DNA topoisomerase I of tumors and suppresses the proliferation of cancer cells to elicit antitumor effect [24]. Studies in animal and human subjects have shown that 10-hydroxycamptothecin (HCPT) is more potent and less toxic than the parent compound CPT. Casticin is a polymethylflavone isolated from a traditional Chinese therapeutic plant named Vitex trifolia L. from the Verbenaceae family [25]. The plant contributes to improve many morbidities including premenstrual syndrome, mastalgia, inflammation and sexual dysfunction, and also helps to relieve pain, and possesses antinociceptive effects. This plant is useful in mild hyperprolactinemia and luteal phase defects. It is also helpful in alleviating menstruation, bleeding management uterine fibroids, polycystic ovarian syndrome, prostate disorders, migrainous women with premenstrual syndrome [26]. Casticin is a flavonoid compound found in several medicinal plants, including Vitex agnus-castus (chaste tree). It has been investigated for its various potential health benefits. Research suggests that casticin possesses anti-inflammatory and antioxidant properties, which may help reduce inflammation and oxidative stress in the body. This could potentially benefit conditions such as arthritis and cardiovascular disease. Some studies also indicate that casticin may have anticancer properties, inhibiting the growth and proliferation of cancer cells in certain types of cancer.

This flavonoid compound is found in various fruits and vegetables and has been studied for its potential health-promoting effects. Like other flavonoids, 3',5'-dihydroxyflavanone exhibits antioxidant properties, which can help protect cells from oxidative damage and reduce the risk of chronic diseases such as heart disease and cancer. Additionally, some research suggests that this compound may have anti-inflammatory properties, which could help alleviate inflammation-related conditions such as arthritis and inflammatory bowel disease. This flavonoid compound is also found in various plants and has been investigated for its potential health benefits. Like other flavonoids, (2S)-2',7-Dimethoxy-3',5'-dihydroxy flavanone possesses antioxidant properties, which can help protect cells from oxidative damage and reduce the risk of chronic diseases. Some research suggests that this compound may also have anti-inflammatory effects, which could potentially benefit conditions such as arthritis and cardiovascular disease. Lupanine is a quinolizidine alkaloid found in various plant species, including lupin seeds. It has been studied for its potential health benefits. Research suggests that Lupanine may have hypotensive (blood pressure-lowering) effects, making it potentially beneficial for individuals with hypertension. Additionally, Lupanine has been investigated for its potential antidiabetic properties, with

some studies indicating that it may help improve insulin sensitivity and glucose metabolism. Flavanones are a class of flavonoid compounds found in various fruits and vegetables, particularly citrus fruits. They have been studied for their numerous health benefits [27].

Flavanones exhibit antioxidant properties, helping to neutralize harmful free radicals in the body and reduce oxidative stress, which is associated with various chronic diseases such as cardiovascular disease and cancer. Some flavanones, such as hesperidin and naringenin, have been shown to have anti-inflammatory effects, which may help reduce inflammation and alleviate symptoms of inflammatory conditions like arthritis. Flavanones have been found to have both antioxidant and anti-inflammatory properties. In particular, different studies have focused their attention on hesperidin and its aglycone form, hesperetin, which play an important role in the prevention of diseases associated with oxidative stress and inflammation, such as cancer and cardiovascular disease [28]. Glabranin is a compound found in licorice (Glycyrrhiza glabra) and has been studied for its potential health benefits. Research suggests that Glabranin may have anti-inflammatory properties, which could help reduce inflammation in the body and alleviate symptoms of inflammatory conditions such as arthritis. Additionally, Glabranin has been investigated for its potential antiviral and antimicrobial properties, which could contribute to its use in traditional medicine for treating infections. Citrinin is a mycotoxin produced by certain fungi, particularly species of Penicillium and Aspergillus. While it is primarily known for its toxic effects, some research has also explored potential health benefits. Limited studies suggest that Citrinin may have antioxidant properties. Glabridin is a flavonoid compound found in licorice root (Glycyrrhiza glabra) and has been studied for its various health benefits. Research suggests that Glabridin may have antioxidant properties, helping to protect cells from oxidative damage and reduce the risk of chronic diseases such as heart disease and cancer. Additionally, Glabridin has been investigated for its potential anti-inflammatory effects, which could help reduce inflammation in the body and alleviate symptoms of inflammatory conditions like arthritis. Glabridin is an isoflavan extracted from licorice (genus Glycyrrhiza) roots, which is also known as a phytoestrogen due to the similarity of its structure and lipophilicity to 17β-estradiol. Studies indicated that glabridin is able to bind to the ERs and induce estrogenic responses in cardiovascular and bone tissues, suggesting its possibility to be used in estrogen replacement therapy.

Mycocyclosin is a compound isolated from certain fungi, particularly marine-derived fungi. It has been studied for its potential pharmaceutical properties. Research suggests that Mycocyclosin may have antibacterial and antifungal properties, making it potentially useful in the development of new antibiotics or antifungal agents. Additionally, some studies indicate that Mycocyclosin may have cytotoxic effects on cancer cells, which could make it a candidate for further investigation as a potential anticancer agent. 2,3-Dehydro-UWM6 is a chemical compound with potential pharmacological applications. Prazepam is a benzodiazepine medication used to treat anxiety and panic disorders. It belongs

to the class of psychoactive drugs known for their anxiolytic (anxiety-reducing), sedative, muscle relaxant, and anticonvulsant properties. Benefits of Prazepam include its ability to alleviate symptoms of anxiety and panic disorders, promote relaxation, and reduce muscle tension. Prazepam is often prescribed for short-term relief of anxiety symptoms and is considered effective when used as directed under medical supervision. (-)-Phaseollinisoflavan is a type of isoflavonoid compound found in certain plants, particularly in legumes like soybeans and chickpeas. Research suggests that isoflavonoids like (-)-Phaseollinisoflavan may have various health benefits, including potential anticancer, antioxidant, and anti-inflammatory properties. Some studies indicate that dietary intake of isoflavonoids may be associated with a reduced risk of certain cancers, such as breast and prostate cancer, as well as cardiovascular disease. Phaseollidin is a natural compound found in certain legumes, including beans and peas. Research suggests that Phaseollidin may have anticancer properties, as it has been shown to inhibit the growth of cancer cells in some studies. Additionally, Phaseollidin may possess anti-inflammatory and antioxidant properties, which could contribute to its potential health benefits.

Glycophymoline is a brand name for a topical solution containing various herbal extracts, including menthol, eucalyptol, and thymol. It is commonly used as a mouthwash and gargle for oral hygiene and minor throat irritations. Benefits may include its antiseptic and refreshing properties, which can help to kill bacteria in the mouth, reduce bad breath, and soothe sore throats. Abscisic acid (ABA) is a plant hormone involved in various physiological processes in plants, such as seed dormancy, bud dormancy, and response to environmental stress. While primarily studied for its role in plants, Abscisic acid (ABA) has also been investigated for its potential health benefits in humans. Research suggests that ABA may have anti-inflammatory, antioxidant, and immunomodulatory effects, which could potentially benefit human health. It has been studied for its potential therapeutic applications in conditions such as diabetes, obesity, inflammation, and autoimmune diseases. Dihydroresveratrol is a derivative of resveratrol, a polyphenolic compound found in various plants, including grapes, berries, and peanuts. Resveratrol and its derivatives have been extensively studied for their potential health benefits, including antioxidant, anti-inflammatory, cardioprotective, neuroprotective, and anticancer properties. While research on alpha-beta-dihydroresveratrol specifically may be limited, it likely shares some of the health-promoting properties of resveratrol due to its structural similarity. Bergaptol is a natural compound found in certain plants, particularly in the citrus family. It is structurally related to bergamottin and is primarily known for its photosensitizing effects. While Bergaptol itself may not have direct health benefits, it is used in combination with other compounds in phototherapy for the treatment of certain skin conditions, such as psoriasis and vitiligo.

Bergapten, also known as 5-methoxypsoralen, is a natural compound found in several plant species, including citrus fruits and certain herbs such as parsley and celery. Bergapten is primarily known for its photosensitizing effects, which have

been utilized in the treatment of skin disorders such as psoriasis, vitiligo, and eczema through a process known as psoralen plus ultraviolet A (PUVA) therapy. Additionally, Bergapten has been studied for its potential anticancer properties, particularly in the treatment of cutaneous T-cell lymphoma (CTCL). Methylarbutin is a derivative of arbutin, a natural compound found in various plant species such as bearberry, cranberry, and blueberry. Arbutin is well-known for its skin-lightening and antioxidant properties. Methylarbutin is often used in cosmetic products for its potential to inhibit melanin production and reduce the appearance of hyperpigmentation, dark spots, and uneven skin tone. Additionally, arbutin and its derivatives like Methylarbutin have been studied for their potential antioxidant and anti-inflammatory effects, which could contribute to their skin-protective properties. Abscisic acid (ABA) is a plant hormone involved in various physiological processes, including seed dormancy, bud dormancy, and response to environmental stress. While primarily studied for its role in plants, Abscisic acid (ABA) has also been investigated for its potential health benefits in humans. Research suggests that Abscisic acid (ABA) may have anti-inflammatory, antioxidant, and immunomodulatory effects, which could potentially benefit human health. It has been studied for its potential therapeutic applications in conditions such as diabetes, obesity, inflammation, and autoimmune diseases.

(+)-8'-Hydroxyabscisic acid is a derivative of abscisic acid (ABA), a plant hormone involved in various physiological processes in plants, including seed dormancy, bud dormancy, and response to environmental stress. While primarily studied for its role in plants, some research suggests that abscisic acid and its derivatives may have potential health benefits in humans. Abscisic acid has been investigated for its potential anti-inflammatory, antioxidant, and immunomodulatory effects, which could potentially benefit human health. It has been studied for its potential therapeutic applications in conditions such as diabetes, obesity, inflammation, and autoimmune diseases. 4-hydroxycoumarin, also known as umbelliferon, is a natural compound found in various plants, including citrus fruits, and is also produced synthetically. Research suggests that 4-hydroxycoumarin may have antioxidant, anti-inflammatory, and antimicrobial properties. It has been studied for its potential use in the treatment of various conditions, including skin disorders, inflammatory diseases, and as a natural sunscreen agent. Scopoletin is a natural coumarin compound found in various plants, including members of the Apiaceae and Rutaceae families. Scopoletin has been studied for its potential pharmacological activities, including antioxidant, anti-inflammatory, antimicrobial, and antitumor properties. It has been investigated for its potential therapeutic applications in conditions such as diabetes, neurodegenerative diseases, cancer, and cardiovascular disorders.

5. Conclusion

In summary, using molecular docking studies, we effectively discovered the

number of compounds present in the LifeGreen™ that have the potential efficacy against breast cancer and uterine fibroids. From the results, we identified that out of 117 compounds that have been extracted from the LC-TOF MS analysis of LifeGreen™, only 34 compounds have the more binding profile against the protein diseases. A total of 22 compounds demonstrated the remarkable capability to bid with all the six protein diseases while the remaining 12 compounds displayed a more selective binding profile, where those only interact with a subset of two to four protein diseases. Finally, the identified 34 compounds, which are associated with breast cancer and uterine fibroids, studied further by conducting comprehensive molecular docking simulations to extract information on their binding affinities and binding site preferences. This study underscores the need for further analytical and experimental studies to establish the safety and efficacy of the identified compounds. In the future, this experiment will be conducted in animal studies for both breast cancer and uterine fibroids using the standard procedure dosage recommended by the WHO and also will proceed with the phytochemical studies in order to identify the similariton between the compounds that have been identified in this paper.

Authors' Contribution

Conceptualization: Ummi Shahieda Lazaroo Binti Zurrein Shah Lazaroo, Chua Kia How. Methodology & Formal analysis: Ummi Shahieda Lazaroo Binti Zurrein Shah Lazaroo. Writing Original Draft: Ummi Shahieda Lazaroo Binti Zurrein Shah Lazaroo, Navanithan Sivanananthan. Discussion & Conclusion: Navanithan Sivanananthan. Writing Review & Editing: Ummi Shahieda Lazaroo Binti Zurrein Shah Lazaroo.

Conflicts of Interest

The authors declare no conflicts of interest regarding the publication of this paper.

References

[1] (2024) LifeGreen™—LifeTree. https://lifetree-asia.com/en/lifegreen/

[2] Cancer Research UK (2024) Cancer Growth Blockers: Targeted Cancer Drugs. https://www.cancerresearchuk.org/about-cancer/treatment/targeted-cancer-drugs/types/cancer-growth-blockers

[3] Donnez, J., Courtoy, G.E. and Dolmans, M.M. (2019) Fibroid Management in Premenopausal Women. *Climacteric*, **22**, 27-33. https://doi.org/10.1080/13697137.2018.1549216

[4] (2024) Uterine Fibroid—Portal MyHEALTH. http://www.myhealth.gov.my/uterine-fibroid/

[5] Levy, B.S. (2008) Modern Management of Uterine Fibroids. *Acta Obstetricia et Gynecologica Scandinavica*, **87**, 812-823. https://doi.org/10.1080/00016340802146912

[6] Bulun, S.E. (2013) Uterine Fibroids. *The New England Journal of Medicine*, **369**,

1344-1355. https://doi.org/10.1056/NEJMra1209993

[7] Navarro, A., Bariani, M.V., Yang, Q. and Al-Hendy, A. (2021) Understanding the Impact of Uterine Fibroids on Human Endometrium Function. *Frontiers in Cell and Developmental Biology*, **9**, Article 633180. https://doi.org/10.3389/fcell.2021.633180

[8] Porter, H.A., Perry, A., Kingsley, C., Tran, N.L. and Keegan, A.D. (2013) IRS1 Is Highly Expressed in Localized Breast Tumors and Regulates the Sensitivity of Breast Cancer Cells to Chemotherapy, While IRS2 Is Highly Expressed in Invasive Breast Tumors. *Cancer Letters*, **338**, 239-248. https://doi.org/10.1016/j.canlet.2013.03.030

[9] Kilpeläinen, T.O., Zillikens, M.C., Stančáková, A., *et al.* (2011) Genetic Variation Near IRS1 Associates with Reduced Adiposity and an Impaired Metabolic Profile. *Nature Genetics*, **43**, 753-760. https://doi.org/10.1038/ng.866

[10] NCI (2024) BRCA Gene Mutations: Cancer Risk and Genetic Testing Fact Sheet. https://www.cancer.gov/about-cancer/causes-prevention/genetics/brca-fact-sheet

[11] Petrucelli, N., Daly, M.B. and Pal, T. (2024) BRCA1- and BRCA2-Associated Hereditary Breast and Ovarian Cancer. GeneReviews. https://www.ncbi.nlm.nih.gov/books/NBK1247/

[12] Lee, M., Cheon, K., Chae, B., *et al.* (2018) Analysis of MED12 Mutation in Multiple Uterine Leiomyomas in South Korean patients. *International Journal of Medical Sciences*, **15**, 124-128. https://doi.org/10.7150/ijms.21856

[13] (2024) Endometriosis. https://www.who.int/news-room/fact-sheets/detail/endometriosis

[14] Nilofer, C., Sukhwal, A., Mohanapriya, A., Sakharkar, M.K. and Kangueane, P. (2020) Small Protein-Protein Interfaces Rich in Electrostatic Are Often Linked to Regulatory Function. *Journal of Biomolecular Structure and Dynamics*, **38**, 3260-3279. https://doi.org/10.1080/07391102.2019.1657040

[15] Shahriar, A. (2023) Organic Carbon-Mineral Interactions with Implications on Water Reuse and Carbon Cycling. https://scholarworks.unr.edu/handle/11714/10828

[16] (2024) LC-TOF-MS. Institut Biologi Sistem. https://www.ukm.my/inbiosis/en/lc-tof-ms/

[17] Vinothkanna, A., Prathiviraj, R., Sivakumar, T.R., Ma, Y. and Sekar, S. (2023) GC-MS and Network Pharmacology Analysis of the Ayurvedic Fermented Medicine, Chandanasava, against Chronic Kidney and Cardiovascular Diseases. *Applied Biochemistry and Biotechnology*, **195**, 2803-2828. https://doi.org/10.1007/s12010-022-04242-7

[18] Ruttkies, C., Neumann, S. and Posch, S. (2019) Improving MetFrag with statistical learning of fragment annotations. *BMC Bioinformatics*, **20**, Article No. 376. https://doi.org/10.1186/s12859-019-2954-7

[19] Daina, A., Michielin, O. and Zoete, V. (2017) SwissADME: A Free Web Tool to Evaluate Pharmacokinetics, Drug-Likeness and Medicinal Chemistry Friendliness of Small Molecules. *Scientific Reports*, **7**, Article No. 42717. https://doi.org/10.1038/srep42717

[20] Alland, C., Moreews, F., Boens, D., *et al.* (2005) RPBS: A Web Resource for Structural Bioinformatics. *Nucleic Acids Research*, **33**, W44-W49. https://doi.org/10.1093/nar/gki477

[21] Volkamer, A., Kuhn, D., Rippmann, F. and Rarey, M. (2012) DoGSiteScorer: A Web Server for Automatic Binding Site Prediction, Analysis and Druggability Assess-

ment. *Bioinformatics*, **28**, 2074-2075. https://doi.org/10.1093/bioinformatics/bts310

[22] Mandal, D., Mukherjee, R., Ghosh, S., *et al.* (2023) Small Molecular Antimicrobial Ligands of YspD Are Potential Therapeutic Agents against *Yersinia enterocolitica* Infection. *Proceedings of the National Academy of Sciences, India Section B: Biological Sciences*, **93**, 461-471. https://doi.org/10.1007/s40011-022-01443-2

[23] Li, Q., Liu, C., Zhao, X., *et al.* (2011) Preparation, Characterization and Targeting of Micronized 10-Hydroxycamptothecin-Loaded Folate-Conjugated Human Serum Albumin Nanoparticles to Cancer Cells. *International Journal of Nanomedicine*, **6**, 397-405. https://doi.org/10.2147/IJN.S16144

[24] Song, M., Yin, S., Zhao, R., *et al.* (2019) (S)-10-Hydroxycamptothecin Inhibits Esophageal Squamous Cell Carcinoma Growth *in Vitro* and *in Vivo via* Decreasing Topoisomerase I Enzyme Activity. *Cancers*, **11**, Article 1964. https://doi.org/10.3390/cancers11121964

[25] Lorence, A., Medina-Bolivar, F. and Nessler, C.L. (2004) Camptothecin and 10-Hydroxycamptothecin from *Camptotheca acuminata* Hairy Roots. *Plant Cell Reports*, **22**, 437-441. https://doi.org/10.1007/s00299-003-0708-4

[26] Rafieian-Kopaei, M. and Movahedi, M. (2017) Systematic Review of Premenstrual, Postmenstrual and Infertility Disorders of Vitex Agnus Castus. *EElectronic Physician*, **9**, 3685-3689. https://doi.org/10.19082/3685

[27] Wiedemann, M., Gurrola-Díaz, C.M., Vargas-Guerrero, B., Wink, M., García-López, P.M. and Düfer, M. (2015) Lupanine Improves Glucose Homeostasis by Influencing KATP Channels and Insulin Gene Expression. *Molecules*, **20**, 19085-19100. https://doi.org/10.3390/molecules201019085

[28] Khan, A., Ikram, M., Hahm, J.R. and Kim, M.O. (2020) Antioxidant and Anti-Inflammatory Effects of Citrus Flavonoid Hesperetin: Special Focus on Neurological Disorders. *Antioxidants*, **9**, Article 609. https://doi.org/10.3390/antiox9070609

Appendix

Table A1. Shows compound spectrum result list which consist of all the details from LC-TOF-MS analysis.

M/Z PEAK HIT	*GRAPH M/Z OVER INTENSITY (PEAK NO)*	*RT (MIN)*	*AREA*	*SIGNAL TO NOISE RATION (S/N)*	*PRECURSOR M/Z (CHROMATOGRAM)*	*FRAGMENTATION (INTENSITY)*	*COLLISION ENERGY (Ev)*	*MOLECULAR FORMULA*	*Mono isotopic Mass*
218.9853	13	1.4	78569	66.7	AutoMSn (242.0010)	182.9641 598 190.9905 1277 200.9748 1325 201.9746 330 218.9853 13669 219.9862 3437 220.9840 1614 242.0023 2244 243.0023 616 265.0179 314	22.1	$C_7H_6O_6S$	217.989
325.1181	15	1.9	49668	73	AutoMSn (309.1324)	117.0562 449 127.0402 1207 130.0530 166 145.0506 779 148.0623 194 163.0622 148 225.0879 188 226.0734 192 274.0966 220 292.1116 313	25.5	$C_{20}H_{20}O_4$	324.136
163.0609	21	2	79661	88.6	AutoMSn (365.1092)	185.0435 195 203.0524 417 365.1107 521		$C_6H_{10}O_5$	162.053
136.064	39	2.6	29720	70.1	AutoMSn (268.1092)	115.0393 134 119.0369 254 133.0525 263 136.0640 26078 137.0649 1163 268.1101 1319		C_8H_9NO	135.068
215.0195	45	3	44717	70.9	AutoMSn (130.0523)	130.0525 5009 163.0611 904 175.0267 1013 193.0369 2962 215.0195 11372 230.9944 2343 259.0974 1813 291.0178 2990 322.0834 2695 407.0505 4487		$C_6H_6N_4O_3S$	214.016

251.0943	65	7.3	247093	887.7	AutoMSn (310.1649)	147.0476 786 175.0395 4262 176.0436 370 207.0649 7163 208.0668 876 236.0678 1165 251.0943 215671 252.0974 23390 253.0976 1821 310.1664 1449		$C_{13}H_{14}O_5$	250.084 1236
295.1332	69	7.6	297019	549	AutoMSn (589.2497)	120.0817 4190 180.1027 40659 181.1057 4225 200.0714 3809 235.1091 36428 236.1120 4538 260.0937 11591 277.1198 6738 295.1321 29595 296.1337 4089		$C_{14}H_{18}N_2O_5$	294.122
114.0925	97	9.1	410677	766.7	AutoMSn (340.2600)	114.0925 94001 115.0948 6098 209.1659 22605 226.1919 10772 227.1785 8580 228.1615 15199 322.2517 14478 340.2634 5283 435.3349 6041 453.3465 6718		$C_6H_{11}NO$	113.084
183.0787	111	9.5	34410	97.2	AutoMSn (290.2694)	118.0919 111 122.0829 442 242.2479 2983 243.2535 413 272.2650 272 288.2918 397 289.2902 120 290.2724 5694 291.2730 948		$C_9H_{10}O_4$	182.058
325.1181	15	1.9	49668	73	AutoMSn (309.1324)	117.0562 449 127.0402 1207 130.0530 166 145.0506 779 148.0623 194 163.0622 148 225.0879 188 226.0734 192 274.0966 220 292.1116 313	25.5	$C_{20}H_{20}O_4$	324.136

325.1181	15	1.9	49668	73	AutoMSn (309.1324)	117.0562 449 127.0402 1207 130.0530 166 145.0506 779 148.0623 194 163.0622 148 225.0879 188 226.0734 192 274.0966 220 292.1116 313	25.5	$C_{20}H_{20}O_4$	324.136
325.1181	15	1.9	49668	73	AutoMSn (309.1324)	117.0562 449 127.0402 1207 130.0530 166 145.0506 779 148.0623 194 163.0622 148 225.0879 188 226.0734 192 274.0966 220 292.1116 313	25.5	$C_{18}H_{16}N_2O_4$	324.111
325.1181	15	1.9	49668	73	AutoMSn (309.1324)	117.0562 449 127.0402 1207 130.0530 166 145.0506 779 148.0623 194 163.0622 148 225.0879 188 226.0734 192 274.0966 220 292.1116 313	25.5	$C_{19}H_{16}O_5$	324.1
325.1181	15	1.9	49668	73	AutoMSn (309.1324)	117.0562 449 127.0402 1207 130.0530 166 145.0506 779 148.0623 194 163.0622 148 225.0879 188 226.0734 192 274.0966 220 292.1116 313	25.5	$C_{19}H_{17}ClN_2O$	324.103
325.1181	15	1.9	49668	73	AutoMSn (309.1324)	117.0562 449 127.0402 1207 130.0530 166 145.0506 779 148.0623 194 163.0622 148 225.0879 188 226.0734 192 274.0966 220 292.1116 313	25.5	$C_{20}H_{20}O_4$	324.136

325.1181	15	1.9	49668	73	AutoMSn (309.1324)	117.0562 449 127.0402 1207 130.0530 166 145.0506 779 148.0623 194 163.0622 148 225.0879 188 226.0734 192 274.0966 220 292.1116 313	25.5	$C_{20}H_{20}O_4$	324.136
325.1181	15	1.9	49668	73	AutoMSn (309.1324)	117.0562 449 127.0402 1207 130.0530 166 145.0506 779 148.0623 194 163.0622 148 225.0879 188 226.0734 192 274.0966 220 292.1116 313	25.5	$C_{12}H_{20}O_{10}$	324.106
325.1181	15	1.9	49668	73	AutoMSn (309.1324)	117.0562 449 127.0402 1207 130.0530 166 145.0506 779 148.0623 194 163.0622 148 225.0879 188 226.0734 192 274.0966 220 292.1116 313	25.5	$C_{12}H_{20}O_{10}$	324.106
163.0609	21	2	79661	88.6	AutoMSn (365.1092)	185.0435 195 203.0524 417 365.1107 521		$C_6H_{10}O_5$	162.053
163.0609	21	2	79661	88.6	AutoMSn (365.1092)	185.0435 195 203.0524 417 365.1107 521		$C_6H_{10}O_5$	162.053
163.0609	21	2	79661	88.6	AutoMSn (365.1092)	185.0435 195 203.0524 417 365.1107 521		$C_6H_{10}O_5$	162.053
163.0609	21	2	79661	88.6	AutoMSn (365.1092)	185.0435 195 203.0524 417 365.1107 521		$C_6H_{10}O_5$	162.053
163.0609	21	2	79661	88.6	AutoMSn (365.1092)	185.0435 195 203.0524 417 365.1107 521		$C_6H_{10}O_5$	162.053
163.0609	21	2	79661	88.6	AutoMSn (365.1092)	185.0435 195 203.0524 417 365.1107 521		$C_6H_{10}O_5$	162.053

163.0609	21	2	79661	88.6	AutoMSn (365.1092)	185.0435 195 203.0524 417 365.1107 521		$C_{10}H_{10}O_2$	162.068
163.0609	21	2	79661	88.6	AutoMSn (365.1092)	185.0435 195 203.0524 417 365.1107 521		$C_{10}H_{10}O_2$	162.068
163.0609	21	2	79661	88.6	AutoMSn (365.1092)	185.0435 195 203.0524 417 365.1107 521		$C_{10}H_{10}O_2$	162.068
136.064	39	2.6	29720	70.1	AutoMSn (268.1092)	115.0393 134 119.0369 254 133.0525 263 136.0640 26078 137.0649 1163 268.1101 1319		$C_4H_9NO_4$	135.053
136.064	39	2.6	29720	70.1	AutoMSn (268.1092)	115.0393 134 119.0369 254 133.0525 263 136.0640 26078 137.0649 1163 268.1101 1319		C_8H_9NO	135.068
136.064	39	2.6	29720	70.1	AutoMSn (268.1092)	115.0393 134 119.0369 254 133.0525 263 136.0640 26078 137.0649 1163 268.1101 1319		$C_4H_9NO_4$	135.053
136.064	39	2.6	29720	70.1	AutoMSn (268.1092)	115.0393 134 119.0369 254 133.0525 263 136.0640 26078 137.0649 1163 268.1101 1319		C_8H_9NO	135.068
136.064	39	2.6	29720	70.1	AutoMSn (268.1092)	115.0393 134 119.0369 254 133.0525 263 136.0640 26078 137.0649 1163 268.1101 1319		$C_5H_5N_5$	135.054
136.064	39	2.6	29720	70.1	AutoMSn (268.1092)	115.0393 134 119.0369 254 133.0525 263 136.0640 26078 137.0649 1163 268.1101 1319		C_8H_9NO	135.068

136.064	39	2.6	29720	70.1	AutoMSn (268.1092)	115.0393 134 119.0369 254 133.0525 263 136.0640 26078 137.0649 1163 268.1101 1319		C_8H_9NO	135.068
215.0195	45	3	44717	70.9	AutoMSn (130.0523)	130.0525 5009 163.0611 904 175.0267 1013 193.0369 2962 215.0195 11372 230.9944 2343 259.0974 1813 291.0178 2990 322.0834 2695 407.0505 4487		$C_{12}H_6O_4$	214.027
215.0195	45	3	44717	70.9	AutoMSn (130.0523)	130.0525 5009 163.0611 904 175.0267 1013 193.0369 2962 215.0195 11372 230.9944 2343 259.0974 1813 291.0178 2990 322.0834 2695 407.0505 4487		$C_5H_{11}O_7P$	214.024
215.0195	45	3	44717	70.9	AutoMSn (130.0523)	130.0525 5009 163.0611 904 175.0267 1013 193.0369 2962 215.0195 11372 230.9944 2343 259.0974 1813 291.0178 2990 322.0834 2695 407.0505 4487		$C_5H_{11}O_7P$	214.024
215.0195	45	3	44717	70.9	AutoMSn (130.0523)	130.0525 5009 163.0611 904 175.0267 1013 193.0369 2962 215.0195 11372 230.9944 2343 259.0974 1813 291.0178 2990 322.0834 2695 407.0505 4487		$C_5H_{11}O_7P$	214.024

215.0195	45	3	44717	70.9	AutoMSn (130.0523)	130.0525 5009 163.0611 904 175.0267 1013 193.0369 2962 215.0195 11372 230.9944 2343 259.0974 1813 291.0178 2990 322.0834 2695 407.0505 4487		$C_5H_{11}O_7P$	214.024
215.0195	45	3	44717	70.9	AutoMSn (130.0523)	130.0525 5009 163.0611 904 175.0267 1013 193.0369 2962 215.0195 11372 230.9944 2343 259.0974 1813 291.0178 2990 322.0834 2695 407.0505 4487		$C_7H_6N_2O_6$	214.023
251.0943	65	7.3	247093	887.7	AutoMSn (310.1649)	147.0476 786 175.0395 4262 176.0436 370 207.0649 7163 208.0668 876 236.0678 1165 251.0943 215671 252.0974 23390 253.0976 1821 310.1664 1449		$C_{10}H_{18}O_5S$	250.087
251.0943	65	7.3	247093	887.7	AutoMSn (310.1649)	147.0476 786 175.0395 4262 176.0436 370 207.0649 7163 208.0668 876 236.0678 1165 251.0943 215671 252.0974 23390 253.0976 1821 310.1664 1449		$C_{10}H_{18}O_5S$	250.087
251.0943	65	7.3	247093	887.7	AutoMSn (310.1649)	147.0476 786 175.0395 4262 176.0436 370 207.0649 7163 208.0668 876 236.0678 1165 251.0943 215671 252.0974 23390 253.0976 1821 310.1664 1449		$C_{16}H_{14}N_2O$	250.111

251.0943	65	7.3	247093	887.7	AutoMSn (310.1649)	147.0476 786 175.0395 4262 176.0436 370 207.0649 7163 208.0668 876 236.0678 1165 251.0943 215671 252.0974 23390 253.0976 1821 310.1664 1449		$C_{16}H_{14}N_2O$	250.111
251.0943	65	7.3	247093	887.7	AutoMSn (310.1649)	147.0476 786 175.0395 4262 176.0436 370 207.0649 7163 208.0668 876 236.0678 1165 251.0943 215671 252.0974 23390 253.0976 1821 310.1664 1449		$C_{17}H_{14}O_2$	250.099
251.0943	65	7.3	247093	887.7	AutoMSn (310.1649)	147.0476 786 175.0395 4262 176.0436 370 207.0649 7163 208.0668 876 236.0678 1165 251.0943 215671 252.0974 23390 253.0976 1821 310.1664 1449		$C_{16}H_{14}N_2O$	250.111
251.0943	65	7.3	247093	887.7	AutoMSn (310.1649)	147.0476 786 175.0395 4262 176.0436 370 207.0649 7163 208.0668 876 236.0678 1165 251.0943 215671 252.0974 23390 253.0976 1821 310.1664 1449		$C_{15}H_{10}N_2O_2$	250.074
251.0943	65	7.3	247093	887.7	AutoMSn (310.1649)	147.0476 786 175.0395 4262 176.0436 370 207.0649 7163 208.0668 876 236.0678 1165 251.0943 215671 252.0974 23390 253.0976 1821 310.1664 1449		$C_{16}H_{14}N_2O$	250.111

295.1332	69	7.6	297019	549	AutoMSn (589.2497)	120.0817 4190 180.1027 40659 181.1057 4225 200.0714 3809 235.1091 36428 236.1120 4538 260.0937 11591 277.1198 6738 295.1321 29595 296.1337 4089		$C_{12}H_{19}N_6OP$	294.136
295.1332	69	7.6	297019	549	AutoMSn (589.2497)	120.0817 4190 180.1027 40659 181.1057 4225 200.0714 3809 235.1091 36428 236.1120 4538 260.0937 11591 277.1198 6738 295.1321 29595 296.1337 4089		$C_{18}H_{18}N_2O_2$	294.137
295.1332	69	7.6	297019	549	AutoMSn (589.2497)	120.0817 4190 180.1027 40659 181.1057 4225 200.0714 3809 235.1091 36428 236.1120 4538 260.0937 11591 277.1198 6738 295.1321 29595 296.1337 4089		$C_{18}H_{18}N_2O_2$	294.137
295.1332	69	7.6	297019	549	AutoMSn (589.2497)	120.0817 4190 180.1027 40659 181.1057 4225 200.0714 3809 235.1091 36428 236.1120 4538 260.0937 11591 277.1198 6738 295.1321 29595 296.1337 4089		$C_{10}H_{18}N_2O_8$	294.106
295.1332	69	7.6	297019	549	AutoMSn (589.2497)	120.0817 4190 180.1027 40659 181.1057 4225 200.0714 3809 235.1091 36428 236.1120 4538 260.0937 11591 277.1198 6738 295.1321 29595 296.1337 4089		$C_{19}H_{18}O_3$	294.126

295.1332	69	7.6	297019	549	AutoMSn (589.2497)	120.0817 4190 180.1027 40659 181.1057 4225 200.0714 3809 235.1091 36428 236.1120 4538 260.0937 11591 277.1198 6738 295.1321 29595 296.1337 4089		$C_{15}H_{18}O_6$	294.11
183.0787	111	9.5	34410	97.2	AutoMSn (290.2694)	118.0919 111 122.0829 442 242.2479 2983 243.2535 413 272.2650 272 288.2918 397 289.2902 120 290.2724 5694 291.2730 948		$C_9H_{10}O_4$	182.058
183.0787	111	9.5	34410	97.2	AutoMSn (290.2694)	118.0919 111 122.0829 442 242.2479 2983 243.2535 413 272.2650 272 288.2918 397 289.2902 120 290.2724 5694 291.2730 948		$C_9H_{10}O_4$	182.058
183.0787	111	9.5	34410	97.2	AutoMSn (290.2694)	118.0919 111 122.0829 442 242.2479 2983 243.2535 413 272.2650 272 288.2918 397 289.2902 120 290.2724 5694 291.2730 948		$C_9H_{10}O_4$	182.058
183.0787	111	9.5	34410	97.2	AutoMSn (290.2694)	118.0919 111 122.0829 442 242.2479 2983 243.2535 413 272.2650 272 288.2918 397 289.2902 120 290.2724 5694 291.2730 948		$C_9H_{10}O_4$	182.058

183.0787	111	9.5	34410	97.2	AutoMSn (290.2694)	118.0919 111 122.0829 442 242.2479 2983 243.2535 413 272.2650 272 288.2918 397 289.2902 120 290.2724 5694 291.2730 948		$C_9H_{10}O_4$	182.058
183.0787	111	9.5	34410	97.2	AutoMSn (290.2694)	118.0919 111 122.0829 442 242.2479 2983 243.2535 413 272.2650 272 288.2918 397 289.2902 120 290.2724 5694 291.2730 948		$C_9H_{10}O_4$	182.058
183.0787	111	9.5	34410	97.2	AutoMSn (290.2694)	118.0919 111 122.0829 442 242.2479 2983 243.2535 413 272.2650 272 288.2918 397 289.2902 120 290.2724 5694 291.2730 948		$C_9H_{10}O_4$	182.058
183.0787	111	9.5	34410	97.2	AutoMSn (290.2694)	118.0919 111 122.0829 442 242.2479 2983 243.2535 413 272.2650 272 288.2918 397 289.2902 120 290.2724 5694 291.2730 948		$C_6H_{14}O_6$	182.079
183.0787	111	9.5	34410	97.2	AutoMSn (290.2694)	118.0919 111 122.0829 442 242.2479 2983 243.2535 413 272.2650 272 288.2918 397 289.2902 120 290.2724 5694 291.2730 948		$C_6H_{14}O_6$	182.079